Supporting Information

Comprehensive fragment screening of the SARS-CoV-2 proteome explores novel chemical space for drug development

Hannes Berg,[a,b‡] Maria A. Wirtz Martin,[a,b‡] Nadide Altincekic,[a,b‡] Islam Alshamleh,[a,b] Jasleen Kaur Bains,[a,b] Julius Blechar,[a] Betül Ceylan,[a,b] Vanessa de Jesus,[a,b] Karthikeyan Dhamotharan,[b,c] Christin Fuks,[a] Santosh L. Gande,[a,b] Bruno Hargittay,[a,b] Katharina F. Hohmann,[a,b] Marie T. Hutchison,[a,b] Sophie Marianne Korn,[b,c] Robin Krishnathas,[a,b] Felicitas Kutz,[a,b] Verena Linhard,[a,b] Tobias Matzel,[a,b] Nathalie Meiser,[a] Anna Niesteruk,[a,b] Dennis J. Pyper,[a,b] Linda Schulte,[a,b] Sven Trucks,[a] Kamal Azzaoui,[d] Marcel J. J. Blommers,[d] Yojana Gadiya,[e,f] Reagon Karki,[e,f] Andrea Zaliani,[e,f] Philip Gribbon,[e,f] Marcius da Silva Almeida,[g,h] Cristiane Dinis Anobom,[i,j] Anna L. Bula,[k] Matthias Bütikofer,[l] Ícaro Putinhon Caruso,[g,m] Isabella Caterina Felli,[n,o] Andrea T. Da Poian,[g] Gisele Cardoso de Amorim,[g,p] Nikolaos K. Fourkiotis,[q] Angelo Gallo,[q,r] Dhiman Ghosh,[l] Francisco Gomes-Neto,[i,s] Oksana Gorbatyuk,[t] Bing Hao,[t] Vilius Kurauskas,[u] Lauriane Lecoq,[v] Yunfeng Li,[t] Nathane Cunha Mebus-Antunes,[g] Miguel Mompeán,[w] Thais Cristtina Neves-Martins,[g] Martí Ninot-Pedrosa,[v] Anderson S. Pinheiro,[j] Letizia Pontoriero,[n,o] Yulia Pustovalova,[t] Roland Riek,[l] Angus J. Robertson,[x] Marie Jose Abi Saad,[y] Miguel Á. Treviño,[w] Aikaterini C. Tsika,[q] Fabio C. L. Almeida,[g,i] Ad Bax,[x] Katherine Henzler-Wildman,[u] Jeffrey C. Hoch,[t] Kristaps Jaudzems,[k] Douglas V. Laurents,[w] Julien Orts,[y] Roberta Pierattelli,[n,o] Georgios A. Spyroulias,[q] Elke Duchardt-Ferner,[b,c] Jan Ferner,[a,b] Boris Fürtig,[a,b] Martin Hengesbach,[a] Frank Löhr,[b,c] Nusrat Qureshi,[a,b] Christian Richter,[a,b] Krishna Saxena,[a,b] Andreas Schlundt,[b,c] Sridhar Sreeramulu,[a,b] Anna Wacker,[a,b] Julia E. Weigand,[z] Julia Wirmer-Bartoschek,[a,b] Jens Wöhnert,[b,c] and Harald Schwalbe*[a,b]

‡ These authors contributed equally to this work.

*Correspondence: Harald Schwalbe schwalbe@nmr.uni-frankfurt.de

Material and Methods:

We recorded ^{1}H 1D spectra at T=298 K at a ratio of each ligand to one protein target of 20:1. 190 µl of a 10 µM protein in screening buffer (25 mM NaPi, 150 mM NaCl, pH 7.5) was manually pipetted into 3 mm NMR tubes. 10 µl of the fragment mixture was added using a pipetting robot to a final concentration of 200 µM for each fragment. During the screen, sample mixes were stored at 4 °C. The experiments were conducted at a 600 MHz NMR spectrometer equipped with a cryoprobe. For the NMR measurements, 5% DMSO was used for locking the NMR spectrometer frequency. Shim optimization was performed on the H_2O signal by using a home-built script for ^{1}H gradient shimming. In screening experiments (Supporting Information Table 5), the residual water signal was suppressed using the SOGGY sequence, which was implemented in all screening pulse sequences. From our experience, application of the composite water pulse makes this method more robust than conventional excitation sculpting in case of air bubbles in the NMR tube or tubes with smaller filling height. Two mixing times (5 ms, 100 ms) with a bandwidth of the CPMG-pulse of 6.25 kHz were recorded for ^{1}H-R_2-CPMG experiments. R_2-CPMG pulse sequences were performed using temperature compensation. For the STD experiments, all parameters were optimized using a standard sample (Supporting Information Figure - 26). All these experiments detected changes of ligand signals in the presence of sub-stoichiometric protein target.

nsp10•nsp14: Samples for fragment screening were prepared in 3 mm NMR tubes and contained mixtures of eight fragments dissolved at 250 µM concentration each in 20 mM potassium phosphate buffer (pH 8.0) with 500 mM NaCl, 0.5 mM DTT, 0.5 mM $MgCl_2$, 4% DMSO-d_6 and 10% D_2O. Nsp14•nsp10 complex was added at 12.5 µM concentration. 250 µM Sinefungin was used as a known binder for testing of competitive binding to the S-adenosylmethionine binding site.

NMR experiments were performed at 298 K on a 600 MHz Bruker Avance Neo spectrometer equipped with a QCI-F quadruple-resonance pulsed-field-gradient cryoprobe. Proton 1D, CPMG (T2), and waterLOGSY spectra were recorded for each sample in the absence and presence of Nsp14-Nsp10, as well as after the addition of the competitive binder. The waterLOGSY spectra were acquired with 128 scans and a mixing time of 1.7 s. Water suppression was achieved using excitation sculpting with gradients, and protein signals were filtered using a 30 ms trim pulse. The CPMG (T2) spectra were acquired with 128 scans, water signal presaturation during the relaxation delay, and a spin-lock time of 400 ms.

Ligand Observed Titration

A separate 200 µL sample was prepared for each step of the titration. Each contained 50 µM ligand and varying protein (ORF9a (NTD), nsp3c (SUD-MC), and nsp5) concentrations between 0 - 500 µM in the screening buffer (25 mM Sodium Phosphate, 150 mM NaCl, pH 7.5 with 5% d6-DMSO). 100 µM DSS was used as an internal reference. Depending on the solubility and availability of the different proteins, different concentrations and number of steps were used for the titrations. With the ligand concentration fixed to 50 µM, the ORF9a (NTD) concentration was varied in the following steps: 0, 50, 100, 200, 350, 500 µM. With the ligand concentration fixed to 50 µM, the nsp3c (SUD-MC) concentration was varied in the following steps: 0, 50, 100, 150, 200, 250, 279 µM. With the ligand concentration fixed to 50 µM, the nsp5 concentration was varied in the following steps: 0, 50, 100, 150, 200, 250, 300, 350, 400, 450, 500, 550, 577 µM. Additionally, a titration with 5 µM ligand concentration with the following steps was used for nsp5: 0, 5, 10, 20, 30, 50, 75, 100, 125, 150, 175, 200 µM. ^{1}D-^{1}H NMR measurements were carried out in 1.7 mm NMR-tubes in a 600 MHz spectrometer at 298 K. Fitting was performed with a one-site-specific binding model ($Y = Bmax * X/(Kd + X)$), where X is the concentration of the ligand and Y is the chemical shift difference.

Protein Observed Titration

A separate 550 µL sample was prepared for each step of the titration. Each contained 50 µM nsp10 and varying ligand concentrations between 0 - 2 mM in the screening buffer (25 mM Sodium Phosphate,

150 mM NaCl, pH 7.5 with 5% d6-DMSO). 10 µM DSS was used as an internal reference. With the protein concentration fixed to 50 µM, the ligand concentration was varied in the following steps: 0, 50, 100, 200, 400, 1000, 2000 µM. $^{1}H^{15}N$-BEST-TROSY NMR measurements were carried out in 5 mm NMR-tubes in a 600 MHz spectrometer at 298 K. The previous assignment of nsp10 was overlayed with the TROSY spectra to identify the peaks. Fitting was performed as mentioned above.

For the nsp5 titration, 100 µM of uniformly ^{15}N labeled nsp5 was titrated with 0 – 2 mM of the ligand in 50 mM NaPi (pH 7.0), 0.5 mM TCEP, 10% D_2O, and 0 – 2% d6-DMSO. The titration steps were 0, 1, 2, 4, 8, 12, 16, and 20 equivalent of ligand over protein. All experiments were performed at a temperature of 298 K.

FTMAP analysis, PDBsum, and autodock

For the FTMap analysis, the corresponding PDB codes and possible restrictions regarding chains (chain a or chain b for example) were entered and uploaded to the FTMap web service. After the analysis had finished, the text file and the pymol file containing the cross-cluster information were downloaded for further analyzation. The amino acid sequence for the highest volume clefts was extracted using PDBsum. This sequence was then colored in the pymol file of the FTMap analysis, giving an indication of the position of these clefts on the protein. After this, it was possible to ascertain which cross-cluster was binding in which cleft of the protein. With this information and the cheminformatic characterization of the 768 compounds from the library according to the 16 FTMap probes, analyzing the coverage between the FTMap probes of a binder from the screening and the occurrence of these same probes in any given cross-clusters of a cleft. If, for example, cleft 2 was identified to be the main binding site in nsp10, cross-clusters 0, 3, 5, and 6 could be identified to be occupying that space (Supporting Information Figure). Comparing now the FTMap probe characterization of any given binder to the FTMap probes that constitute cross-clusters 0, 3, 5, and 6, gives a percental coverage of the likeness between these two. The higher the percentage is, the more of the probes characterizing the binder are also found in the cross-clusters, up to a coverage of 100%, meaning all the binder probes are also present in the cross-cluster. This gives the possibility to filter the NMR binders of one protein according to their coverage in the identified cross-cluster of a protein cleft. After filtering the NMR binders according to their coverage of the cleft cross-clusters, one binder per protein was docked using Swissdock's web server without any experimental restraints. For 50% of the targets, the top ranked pose occupied the same cleft that was seen in the PDBsum and FTMap analysis. For the rest of the targets, using the NMR data as additional information, an orientation was chosen that also occupied the clefts in question.

Similarity/Analog search in ChEMBL and PubChem for NMR ligands

Compounds reported to be active against SARS-CoV-2 viral proteins in target-based screens were identified in the ChEMBL and PubChem Databases. Search criteria for ChEMBL were: 1) Source: 'SARS-CoV-2 Screening Data 2020-21' 2) Confidence Label: 'Direct single protein target assigned' to ensure specificity of the assays. The filtering criteria on PubChem bio-assays were 1) Datasets were published after 2020 2) Bio-assay active compounds were either literature-derived or provided by NCATS (National Center for Advancing Translational Sciences). The identification of active compounds from these sources was done using PubChem's PUG REST API. The KNIME workflow (Supplementary Figure 26) was deployed on these datasets to identify analogues of the hit compounds. The analysis revealed 35 hit fragments associated with 50 analogues identified as active in 16 different SARS-CoV-2 assays, representing a total of 155 distinct bioactivities. The workflow and associated data can be found here https://github.com/Fraunhofer-ITMP/KNIME_NMR

Knowledge graph for NMR data, ChEMBL and PubChem actives

A knowledge graph (KG) was constructed linking the identified ligands targeting 24 viral proteins with the ChEMBL compounds and PubChem actives from our analogue search. Information includes primary mechanism of action of the ChEMBL analogue compounds including target protein and disease indication. The resulting KG consists of 529 nodes and 2352 edges (Supplementary Figure 27). The

codes written to generate the KG can be found at https://github.com/Fraunhofer-ITMP/COVID-NMR-KG.

Tables

Supporting Information Table 1: SCoV2 protein constructs expressed and purified, given with the genomic position and corresponding PDBs for construct design.

Protein *genome position (nt)* [a]	***Trivial name*** Construct expressed	**Size (aa)**[b]	**Boundaries**	**MW [kDa]**	**Sequence (aa)**[c]	**Screening concentration [µM]**
nsp1 *266-805*	***Leader***	**180**		**19.8**	GAMESLVPGFNEKTHVQLSLP VLQVRDVLVRGFGDSVEEVLS EARQHLKDGTCGLVEVEKGVL PQLEQPYVFIKRSDARTAPHGH VMVELVAELEGIQYGRSGETL GVLVPHVGEIPVAYRKVLLRK NGNKGAGGHSYGADLKSFDL GDELGTDPYEDFQENWNTKHS SGVTRELMRELNGG	10
	Globular Domain (GD)	116	13-127	12.7	GAMAHVQLSLPVLQVRDVLV RGFGDSVEEVLSEARQHLKDG TCGLVEVEKGVLPQLEQPYVFI KRSDARTAPHGHVMVELVAEL EGIQYGRSGETLGVLVPHVGEI PVAYRKVLLRKNG	10
nsp2 *806-2,719*		**638**		**70.5**		
	C-terminal Disordered Region (CtDR)	45	557-601	4.9	GKEIIFLEGE TLPTEVLTEE VVLKTGDLQP LEQPTSEAVE APLVGT	10
nsp3 *2,720-8,554*		**1,945**		**217.3**		
a	Ub-like (UBl) domain	111	1-111	12.5	GAMGAPTKVTFGDDTVIEVQ GYKSVNITFELDERIDKVLNEK CSAYTVELGTEVNEFACVVAD AVIKTLQPVSELLTPLGIDLDE WSMATYYLFDESGEFKLASH MYCSFYPPDE	10
b	nsp3b (Macro domain)	170	207-376	18.3	GHMVNSFSGYLKLTDNVYIK NADIVEEAKKVKPTVVVNAA NVYLKHGGGVAGALNKATN NAMQVESDDYIATNGPLKVG GSCVLSGHNLAKHCLHVVGP NVNKGEDIQLLKSAYENFNQH	10

Protein *genome position (nt)* [a]	***Trivial name*** Construct expressed	**Size** **(aa)**[b]	**Boundaries**	**MW [kDa]**	**Sequence** **(aa)**[c]	**Screening concentration** **[µM]**
b	nsp3b·GS-441524	170	207-376	18.3	EVLLAPLLSAGIFGADPIHSLR VCVDTVRTNVYLAVFDKNLY DKLVSSFLEMK GHMVNSFSGYLKLTDNVYIK NADIVEEAKKVKPTVVVNAA NVYLKHGGGVAGALNKATN NAMQVESDDYIATNGPLKVG GSCVLSGHNLAKHCLHVVGP NVNKGEDIQLLKSAYENFNQH EVLLAPLLSAGIFGADPIHSLR VCVDTVRTNVYLAVFDKNLY DKLVSSFLEMK	10 Protein 70 Ligand
c	SUD (SARS-Unique Domain)-N	140	409-548	15.4	GSQDDKKIKACVEEVTTTLEE TKFLTENLLLYIDINGNLHPDS ATLVSDIDITFLKKDAPYIVGD VVQEGVLTAVVIPTKKAGGTT EMLAKALRKVPTDNYITTYPG QGLNGYTVEEAKTVLKKCKS AFYILPSIISNEKQE	10
c	SUD-MC	193	551-743	21.5	GSHMGTVSWNLREMLAHAEE TRKLMPVCVETKAIVSTIQRK YKGIKIQEGVVDYGARFYFYT SKTTVASLINTLNDLNETLVT MPLGYVTHGLNLEEAARYMR SLKVPATVSVSSPDAVTAYNG YLTSSSKTPEEHFIETISLAGSY KDWSYSGQSTQLGIEFLKRGD KSVYYTSNPTTFHLDGEVITFD NLKTLLS	10
d	Papain-like protease PL^{pro}	318	743-1,060	36	SLREVRTIKVFTTVDNINLHTQ VVDMSMTYGQQFGPTYLDGA DVTKIKPHNSHEGKTFYVLPN DDTLRVEAFEYYHTTDPSFLG RYMSALNHTKKWKYPQVNG LTSIKWADNNCYLATALLTLQ QIELKFNPPALQDAYYRARAG EAANFCALILAYCNKTVGELG	10

Protein *genome position (nt)* [a]	***Trivial name*** Construct expressed	**Size** **(aa)**[b]	**Boundaries**	**MW [kDa]**	**Sequence** **(aa)**[c]	**Screening concentration** **[µM]**
e	NAB	116	1,088-1,203	13.4	DVRETMSYLFQHANLDSCKR VLNVVCKTCGQQQTTLKGVE AVMYMGTLSYEQFKKGVQIP CTCGKQATKYLVQQESPFVM MSAPPAQYELKHGTFTCASEY TGNYQCGHYKHITSKETLYCI DGALLTKSSEYKGPITDVFYK ENSYTTTIK GAMGYFTEQPIDLVPNQPYPN ASFDNFKFVCDNIKFADDLNQ LTGYKKPASRELKVTFFPDLN GDVVAIDYKHYTPSFKKGAKL LHKPIVWHVNNATNKATYKP NTWCIRCLWSTKPVET	10
Y		286		31.5	GKRPINPTDQSSYIVDSVTVKN GSIHLYFDKAGQKTYERHSLS HFVNLDNLRANNTKGSLPINV IVFDGKSKCEESSAKSASVYYS QLMCQPILLLDQALVSDVGDS AEVAVKMFDAYVNTFSSTFN VPMEKLKTLVATAEAELAKN VSLDNVLSTFISAARQGFVDS DVETKDVVECLKLSHQSDIEV TGDSCNNYMLTYNKVENMTP RDLGACIDCSARHINAQVAKS HNIALIWNVKDFMSLSEQLRK QIRSAAKKNNLPFKLTCATTR QVVNVVTTKIALKGG	10
nsp5 *10,055-10,972*	***Main protease (M^{pro})***	**306**		**33.8**		
	$_{GS}$nsp5	306	1-306	33.8	GSSGFRKMAFPSGKVEGCMV QVTCGTTTLNGLWLDDVVYC PRHVICTSEDMLNPNYEDLLIR KSNHNFLVQAGNVQLRVIGHS MQNCVLKLKVDTANPKTPKY KFVRIQPGQTFSVLACYNGSPS GVYQCAMRPNFTIKGSFLNGS	10

Protein *genome position (nt)* [a]	***Trivial name*** Construct expressed	**Size (aa)**[b]	**Boundaries**	**MW [kDa]**	**Sequence (aa)**[c]	**Screening concentration [µM]**
					CGSVGFNIDYDCVSFCYMHH MELPTGVHAGTDLEGNFYGPF VDRQTAQAAGTDTTITVNVLA WLYAAVINGDRWFLNRFTTT LNDFNLVAMKYNYEPLTQDH VDILGPLSAQTGIAVLDMCAS LKELLQNGMNGRTILGSALLE DEFTPFDVVRQCSGVTFQGPH HHHHH	
	$_{GHM}$nsp5	306	1-306	33.8	GHMSGFRKMAFPSGKVEGCM VQVTCGTTTLNGLWLDDVVY CPRHVICTSEDMLNPNYEDLLI RKSNHNFLVQAGNVQLRVIG HSMQNCVLKLKVDTANPKTP KYKFVRIQPGQTFSVLACYNG SPSGVYQCAMRPNFTIKGSFL NGSCGSVGFNIDYDCVSFCYM HHMELPTGVHAGTDLEGNFY GPFVDRQTAQAAGTDTTITVN VLAWLYAAVINGDRWFLNRF TTTLNDFNLVAMKYNYEPLT QDHVDILGPLSAQTGIAVLDM CASLKELLQNGMNGRTILGSA LLEDEFTPFDVVRQCSGVTFQ	10
	Full-length	306	1-306	33.8	SGFRKMAFPSGKVEGCMVQV TCGTTTLNGLWLDDVVYCPR HVICTSEDMLNPNYEDLLIRKS NHNFLVQAGNVQLRVIGHSM QNCVLKLKVDTANPKTPKYK FVRIQPGQTFSVLACYNGSPSG VYQCAMRPNFTIKGSFLNGSC GSVGFNIDYDCVSFCYMHHM ELPTGVHAGTDLEGNFYGPFV DRQTAQAAGTDTTITVNVLA WLYAAVINGDRWFLNRFTTT LNDFNLVAMKYNYEPLTQDH VDILGPLSAQTGIAVLDMCAS LKELLQNGMNGRTILGSALLE DEFTPFDVVRQCSGVTFQ	10

Protein *genome position (nt)* [a]	***Trivial name*** Construct expressed	**Size** **(aa)**[b]	**Boundaries**	**MW [kDa]**	**Sequence** **(aa)**[c]	**Screening concentration** **[µM]**
nsp7 *11,843-12,091*		**83**		**9.2**		
	Full-length	83	1-83	9.2	GSKMSDVKCTSVVLLSVLQQL RVESSSKLWAQCVQLHNDILL AKDTTEAFEKMVSLLSVLLSM QGAVDINKLCEEMLDNRATL Q	10
nsp8 *12,092-12,685*		**198**		**21.9**		
	Full-length	198	1-198	21.9	GAIASEFSSLPSYAAFATAQEA YEQAVANGDSEVVLKKLKKS LNVAKSEFDRDAAMQRKLEK MADQAMTQMYKQARSEDKR AKVTSAMQTMLFTMLRKLDN DALNNIINNARDGCVPLNIIPL TTAAKLMVVIPDYNTYKNTC DGTTFTYASALWEIQQVVDA DSKIVQLSEISMDNSPNLAWPL IVTALRANSAVKLQ	9.6
nsp9 *12,686-13,024*		**113**		**12.4**		
	Full-length	113	1-113	12.4	GAMGNNELSPVALRQMSCAA GTTQTACTDDNALAYYNTTK GGRFVLALLSDLQDLKWARFP KSDGTGTIYTELEPPCRFVTDT PKGPKVKYLYFIKGLNNLNRG MVLGSLAATVRLQ	10
nsp10 *13,025-13,441*		**139**		**14.8**		
	Full-length	139	1-139	14.8	MGSDKIHHHHHHAGNATEVP ANSTVLSFCAFAVDAAKAYK DYLASGGQPITNCVKMLCTHT GTGQAITVTPEANMDQESFGG ASCCLYCRCHIDHPNPKGFCD LKGKYVQIPTTCANDPVGFTL	10

Protein *genome position (nt)* [a]	***Trivial name*** Construct expressed	**Size** **(aa)**[b]	**Boundaries**	**MW [kDa]**	**Sequence** **(aa)**[c]	**Screening concentration** **[µM]**
					KNTVCTVCGMWKGYGCSCD QLREPMLQ	
nsp15 *19,621-20,658*	***Endonuclease***	**346**		**38.8**		
	$_{His6}$nsp15	346	1-346	38.8	MGSSHHHHHHSSGENLYFQG HMSLENVAFNVVNKGHFDGQ QGEVPVSIINNTVYTKVDGVD VELFENKTTLPVNVAFELWAK RNIKPVPEVKILNNLGVDIAAN TVIWDYKRDAPAHISTIGVCS MTDIAKKPTETICAPLTVFFDG RVDGQVDLFRNARNGVLITEG SVKGLQPSVGPKQASLNGVTL IGEAVKTQFNYYKKVDGVVQ QLPETYFTQSRNLQEFKPRSQ MEIDFLELAMDEFIERYKLEG YAFEHIVYGDFSHSQLGGLHL LIGLAKRFKESPFELEDFIPMD STVKNYFITDAQTGSSKCVCS VIDLLLDDFVEIIKSQDLSVVS KVVKVTIDYTEISFMLWCKDG HVETFYPKLQ	10
nsp10·nsp16 *20,659-21,552*	***Methyltransferase***	**298**		**33.3**		
	nsp10·**nsp16**	298	1-298	33.3	MGSSHHHHHHSQDPSSQAWQ PGVAMPNLYKMQRMLLEKCD LQNYGDSATLPKGIMMNVAK YTQLCQYLNTLTLAVPYNMR VIHFGAGSDKGVAPGTAVLRQ WLPTGTLLVDSDLNDFVSDAD STLIGDCATVHTANKWDLIISD MYDPKTKNVTKENDSKEGFF TYICGFIQQKLALGGSVAIKIT EHSWNADLYKLMGHFAWWT AFVTNVNASSSEAFLIGCNYL GKPREQIDGYVMHANYIFWR NTNPIQLSSYSLFDMSKFPLKL RGTAVMSLKEGQINDMILSLL SKGRLIIRENNRVVISSDVLVN N	10

Protein *genome position (nt)* [a]	***Trivial name*** Construct expressed	**Size (aa)**[b]	**Boundaries**	**MW [kDa]**	**Sequence (aa)**[c]	**Screening concentration [µM]**
nsp10·nsp14 *18,040-19,620*	**Exoribonuclease**	**527**		**61.4**		
	nsp10·**nsp14**	527	7-527	61.4	MGSSHHHHHHSQDPAENVTG LFKDCSKVITGLHPTQAPTHLS VDTKFKTEGLCVDIPGIPKDM TYRRLISMMGFKMNYQVNGY PNMFITREEAIRHVRAWIGFD VEGCHATREAVGTNLPLQLGF STGVNLVAVPTGYVDTPNNT DFSRVSAKPPPGDQFKHLIPLM YKGLPWNVVRIKIVQMLSDTL KNLSDRVVFVLWAHGFELTS MKYFVKIGPERTCCLCDRRAT CFSTASDTYACWHHSIGFDYV YNPFMIDVQQWGFTGNLQSN HDLYCQVHGNAHVASCDAIM TRCLAVHECFVKRVDWTIEYP IIGDELKINAACRKVQHMVVK AALLADKFPVLHDIGNPKAIK CVPQADVEWKFYDAQPCSDK AYKIEELFYSYATHSDKFTDG VCLFWNCNVDRYPANSIVCRF DTRVLSNLNLPGCDGGSLYVN KHAFHTPAFDKSAFVNLKQLP FFYYSDSPCESHGKQVVSDID YVPLKSATCITRCNLGGAVCR HHANEYRLYLDAYNMMISAG FSLWVYKQFDTYNLWNTFTR LQ	12.5
ORF9a *28,274-29,533*	***Nucleocapsid (N)***	**419**		**45.6**		
	IDR1-NTD- IDR2 (Intrinsically Disordered Region (IDR))	248	1-248	26.5	MSDNGPQNQRNAPRITFGGPS DSTGSNQNGERSGARSKQRRP QGLPNNTASWFTALTQHGKE DLKFPRGQGVPINTNSSPDDQI GYYRRATRRIRGGDGKMKDL SPRWYFYYLGTGPEAGLPYGA NKDGIIWVATEGALNTPKDHI GTRNPANNAAIVLQLPQGTTL PKGFYAEGSRGGSQASSRSSS RSRNSSRNSTPGSSRGTSPARM	10

Protein *genome position (nt)* [a]	***Trivial name*** Construct expressed	**Size (aa)**[b]	**Boundaries**	**MW [kDa]**	**Sequence (aa)**[c]	**Screening concentration [µM]**
	NTD-SR (S/R rich region(SR))	169	44-212	18.1	AGNGGDAALALLLLDRLNQL ESKMSGKGQQQQGQTVTK GLPNNTASWFTALTQHGKED LKFPRGQGVPINTNSSPDDQIG YYRRATRRIRGGDGKMKDLS PRWYFYYLGTGPEAGLPYGA NKDGIIWVATEGALNTPKDHI GTRNPANNAAIVLQLPQGTTL PKGFYAEGSRGGSQASSRSSS RSRNSSRNSTPGSSRGTSPARM AG	10
	NTD	137	44-180	14.9	GLPNNTASWFTALTQHGKED LKFPRGQGVPINTNSSPDDQIG YYRRATRRIRGGDGKMKDLS PRWYFYYLGTGPEAGLPYGA NKDGIIWVATEGALNTPKDHI GTRNPANNAAIVLQLPQGTTL PKGFYAEGSRGGS	9.8
	CTD (C-Terminal Domain)	118	247-364	13.3	GAMGTKKSAAEASKKPRQKR TATKAYNVTQAFGRRGPEQT QGNFGDQELIRQGTDYKHWP QIAQFAPSASAFFGMSRIGME VTPSGTWLTYTGAIKLDDKDP NFKDQVILLNKHIDAYKTFP	10
ORF9b *28,284-28,574*		**97**		**10.8**		
	Full-length	97	1-97	10.8	MDPKISEMHPALRLVDPQIQL AVTRMENAVGRDQNNVGPK VYPIILRLGSPLSLNMARKTLN SLEDKAFQLTPIAVQMTKLAT TEELPDEFVVVTVKSAWSHPQ FEK	11

[a] Genome position in nt corresponding to SCoV2 NCBI reference genome entry NC_045512.2, identical to GenBank entry MN908947.3 (2).
[b] number of amino acids excluding the additional residues due to cloning
[c] additional artificial amino acids due to construct design

Supporting Information Table 2: Screening targets with their corresponding molecular weight and number of binders.

Target	MW [kDa]	Binders
nsp2 (CtDR)	4.92	19
nsp7	9.29	92
ORF9b	11.99	8
nsp9	12.69	2
nsp3e	13.42	21
ORF9a (CTD)	13.56	9
ORF9a (NTD)	14.85	32
nsp3c (SUD-N)	15.54	10
nsp10	16.24	38
ORF9a (NTD-SR)	18.1	5
nsp3b	18.65	10
nsp3b·GS-441524	18.65	5
nsp1	19.9	5
nsp8	21.93	35
nsp3a	23.24	14
ORF9a (IDR1-NTD-IDR2)	26.52	7
nsp3c (SUD-MC)	29.61	154
nsp3y	31.7	81
$_{GS}$nsp5	33.94	12
nsp5	33.8	78
$_{GHM}$nsp5	34.12	38
nsp3d	35.99	150
$_{His6}$nsp15	41.35	42
nsp10·nsp16	51	100
nsp10·nsp14	77.6	44

Supporting Information Table 3: Summary of the 18 proteins and their pdb codes used for the FTMap analysis and the ID of the docked ligand.

Target	**pdb code**	**Manuscript ID**
nsp1	7k7p	1
nsp3e	2k87	39
nsp3a	7kag	61
nsp9	6w4b	30
nsp7	6wiq	65
nsp8	6wiq	112
nsp3c (SUD-N)	2w2g	134
nsp3c (SUD-MC)	2kqv	68
ORF9a (NTD)	6yi3	55
nsp3b	6vxs	41
nsp3d	6w9c	199
His_6nsp15	6w01	115
ORF9a (CTD)	7c22	40
nsp10	6zpe	2
nsp10·nsp16	6w4h	4
ORF9b	6z4u	2
nsp5	6yb7	21
nsp10·nsp14	nsp10·nsp14_modelled	141

Supporting Information Table 4: Summary of the 18 proteins and their FTMap and docking analysis

Target	pdb code	pdb used for analysis	Reason	FTMap (Crossclusters)	Cleft (PDBSum)	Binder Vendor ID	Manuscript ID	NMR result in mixes	Crosscluster Coverage of Binder	Dock Cluster
nsp1	**7k7p**	**7k7p**	**-**	**0, 7**	**Cleft 1**	**Z26365442**	**1**	**WL**	**100, 0**	**20_0**
nsp3e	**2k87**	**2k87**	**SARSCoV 1 used, that's why sequence is not 100% identical**	**1, 4**	**Cleft 3**	**Z136583524**	**39**	**CSP**	**100, 100**	**1_0**
nsp3a	**7kag**	**7kah_chainA**	**Monomer**	**0, 1, 5, 8**	**Cleft 2**	**Z32386228**	**61**	**WL, STD**	**88, 88, 63, 25**	**0_0**
nsp9	**6w4b**	**6w4b_chainA**	**Monomer**	**1, 3**	**Cleft 1**	**Z1374778753**	**30**	**CSP**	**50, 100**	**0_0**
nsp7	**6wiq**	**6wiq_chainA**	**Complex with Nsp8**	**0, 1, 2, 3, 6**	**Cleft 1**	**Z276545932**	**65**	**CSP, STD**	**100, 100, 100, 100, 25**	**1_0**
nsp8	**6wiq**	**6wiq_chainB**	**Complex with Nsp7**	**1, 3, 4, 5, 6**	**Cleft 1**	**Z1349163663**	**112**	**WL, T2, CSP, STD**	**100, 100, 100, 50, 50**	**3_0**
nsp3c (SUD-N)	**2w2g**	**2w2g_screeningConstruct**	**Part of Monomer that was used in Screening**	**0, 2, 4, 5, 6, 9**	**Cleft 1**	**Z57260539**	**134**	**CSP**	**100, 88, 75, 38, 63, 13**	**0_0**
nsp3c (SUD-MC)	**2kqv**	**2kqv**	**-**	**1, 2, 3, 4, 6**	**Cleft 1**	**Z235449082**	**68**	**WL, CSP**	**100, 100, 75, 75, 0**	**0_0**
ORF9a (NTD)	**6yi3**	**6yi3**	**-**	**0, 1, 3, 5, 6, 7**	**Cleft 1**	**Z1250132788**	**55**	**T2, CSP**	**100, 100, 100, 50, 0, 0**	**8_0**
nsp3b	**6vxs**	**6vxs_chainA**	**Monomer**	**0, 1, 2, 3, 5**	**Cleft 1**	**Z52425517**	**41**	**T2, CSP**	**100, 100, 100, 100, 50**	**0_0**
nsp3d	**6w9c**	**6w9c**	**-**	**1, 2, 4**	**Cleft 2**	**Z1741960769**	**199**	**WL, STD**	**75, 75, 75**	**7_0**
$_{His6}$nsp15	**6w01**	**6w01_chainA**	**Monomer**	**1, 2**	**Cleft 1**	**Z71580604**	**115**	**WL, CSP**	**100, 86**	**1_0**
ORF9a (CTD)	**7c22**	**7c22_chainA**	**Dimer**	**1, 2, 6, 8**	**Cleft 1**	**Z145119960**	**40**	**CSP**	**100, 75, 0, 0**	**0_0**
nsp10	**6zpe**	**6zpe_simplified**	**Removed Glycerol**	**0, 3, 5, 6**	**Cleft 1**	**Z336089202**	**2**	**WL, STD**	**100, 83, 33, 33**	**0_0**
nsp10·nsp16	**6w4h**	**6w4h**	**-**	**3, 4, 5, 7, 8, 10**	**Cleft 1**	**Z1891776064**	**4**	**WL, T2, CSP, STD**	**75, 25, 50, 50, 25, 0**	**2_0**
ORF9b	**6z4u**	**6z4u**	**-**	**0, 3, 5**	**Cleft 3**	**Z336089202**	**2**	**WL, STD**	**67, 67, 67**	**0_0**
nsp5	**5r83**	**5r83**	**Removed Ligand**	**1, 2, 7, 8**	**Cleft 2**	**Z44592329**	**21**	**WL, STD**	**100, 33, 33, 33**	**3_0**
nsp10·nsp14	**nsp10·nsp14 _modelled**	**nsp10·nsp14 _modelled**	**Modelled**	**2, 5, 9**	**Cleft 3**	**Z26251905**	**141**	**WL, T2**	**100, 20, 0**	**1_0**

Supporting Information Table 5: Comparison of the 8 overlapping binders of the three different screened nsp5 constructs and their coverage to the different crossclusters occupying the two clefts. The crosscluster 000 corresponds to the main hot spot followed by 001, 002 and so on. FTMap probes from all 8 binders correlate better with crossclusters (crosscluster001, 002) occupying the cleft 2 (active site), suggesting cleft 2 as the putative binding site.

Cleft 2 (Active Site)											
Z-ID	Crosscluster001	% found in cluster	Z-ID	Crosscluster002	% found in cluster	Z-ID	Crosscluster007	% found in cluster	Z-ID	Crosscluster008	% found in cluster
Z979145504	3	75%	Z979145504	3	75%	Z979145504	2	50%	Z979145504	2	50%
Z223388508	5	83%	Z223388508	5	83%	Z223388508	2	33%	Z223388508	2	33%
Z336089202	5	83%	Z336089202	3	50%	Z336089202	2	33%	Z336089202	3	50%
Z933326822	5	83%	Z933326822	3	50%	Z933326822	2	33%	Z933326822	3	50%
Z208334100	6	86%	Z208334100	4	57%	Z208334100	3	43%	Z208334100	3	43%
Z1891776064	3	75%	Z1891776064	2	50%	Z1891776064	1	25%	Z1891776064	3	75%
Z123970702	4	80%	Z123970702	2	40%	Z123970702	2	40%	Z123970702	3	60%
Z31792168	3	60%	Z31792168	4	80%	Z31792168	2	40%	Z31792168	3	60%
Average		78%			61%			37%			53%
Cleft 1											
Z-ID	Crosscluster003	% found in cluster	Z-ID	Crosscluster004	% found in cluster	Z-ID	Crosscluster006	% found in cluster			
Z979145504	3	75%	Z979145504	2	50%	Z979145504	1	25%			
Z223388508	4	67%	Z223388508	3	50%	Z223388508	3	50%			
Z336089202	5	83%	Z336089202	4	67%	Z336089202	2	33%			
Z933326822	5	83%	Z933326822	4	67%	Z933326822	2	33%			
Z208334100	5	71%	Z208334100	4	57%	Z208334100	2	29%			
Z1891776064	3	75%	Z1891776064	2	50%	Z1891776064	1	25%			
Z123970702	3	60%	Z123970702	3	60%	Z123970702	1	20%			
Z31792168	3	60%	Z31792168	3	60%	Z31792168	1	20%			
Average		72%			58%			29%			

Supporting Information Table 6: Comparison of the 6 overlapping nsp5 binders between NMR and X-ray and their corresponding coverage to the different crossclusters occupying the two clefts. The crosscluster 000 corresponds to the main hot spot followed by 001, 002 and so on. FTMap probes from all 6 binders correlate better with crossclusters (crosscluster001, 002) occupying the cleft 2 (active site), suggesting cleft 2 as the putative binding site.

Cleft 2 (Active Site)											
Z-ID	Crosscluster001	% found in cluster	Z-ID	Crosscluster002	% found in cluster	Z-ID	Crosscluster007	% found in cluster	Z-ID	Crosscluster008	% found in cluster
Z219104216	2	67%	Z219104216	2	67%	Z219104216	1	33%	Z219104216	2	67%
Z24758179	6	86%	Z24758179	5	71%	Z24758179	2	29%	Z24758179	3	43%
Z31432226	8	89%	Z31432226	7	78%	Z31432226	3	33%	Z31432226	2	22%
Z31792168	3	60%	Z31792168	4	80%	Z31792168	2	40%	Z31792168	3	60%
Z44592329	3	100%	Z44592329	1	33%	Z44592329	1	33%	Z44592329	1	33%
Z979145504	3	75%	Z979145504	3	75%	Z979145504	2	50%	Z979145504	2	50%
Average		79%			67%			36%			46%
Cleft 1											
Z-ID	Crosscluster003	% found in cluster	Z-ID	Crosscluster004	% found in cluster	Z-ID	Crosscluster006	% found in cluster			
Z219104216	2	67%	Z219104216	2	67%	Z219104216	0	0%			
Z24758179	5	71%	Z24758179	4	57%	Z24758179	3	43%			
Z31432226	6	67%	Z31432226	5	56%	Z31432226	5	56%			
Z31792168	3	60%	Z31792168	3	60%	Z31792168	1	20%			
Z44592329	1	33%	Z44592329	2	67%	Z44592329	1	33%			
Z979145504	3	75%	Z979145504	2	50%	Z979145504	1	25%			
Average		62%			59%			29%			

Supporting Information Table 7: NMR experiments used in the screening of the proteins.

#	NMR experiments*	Sample utilized Solvents	Experiment-specific parameter settings	MT
1	^{1}H 1D	^{1}H 1D with water suppression SOGGY	Excitation sculpting with a composite 180° spin echo pulse. The SOGGY pulse was implemented. NS = 64.	4.5 min
2	water-LOGSY on ^{1}H	waterLOGSY with SOGGY sequence for water suppression	The SOGGY sequence was implemented in the standard waterLOGSY sequence. The mixing time was set to 1.7 ms NS = 320.	27 min
3, 4	T_2 CPMG on ^{1}H	T_2 relaxation using a pseudo2D sequence with CPMG spinlock field of 6.25kHz (5 and 100 ms) with temperature compensation.	The SOGGY sequence was implemented in the standard CPMG sequence. NS = 128.	13 min.
5	*STD*	Offset switch between 0 and -40ppm. Spinlock of 50ms to suppress the protein signals B1 Field of 200 Hz.	Standard sequence with excitation sculpting was used. NS =128	13 min

*Pulse sequence and parameter set for in-house optimized experiments can be obtained upon request and data sets can be downloaded at covid19-nmr.de.

Figures

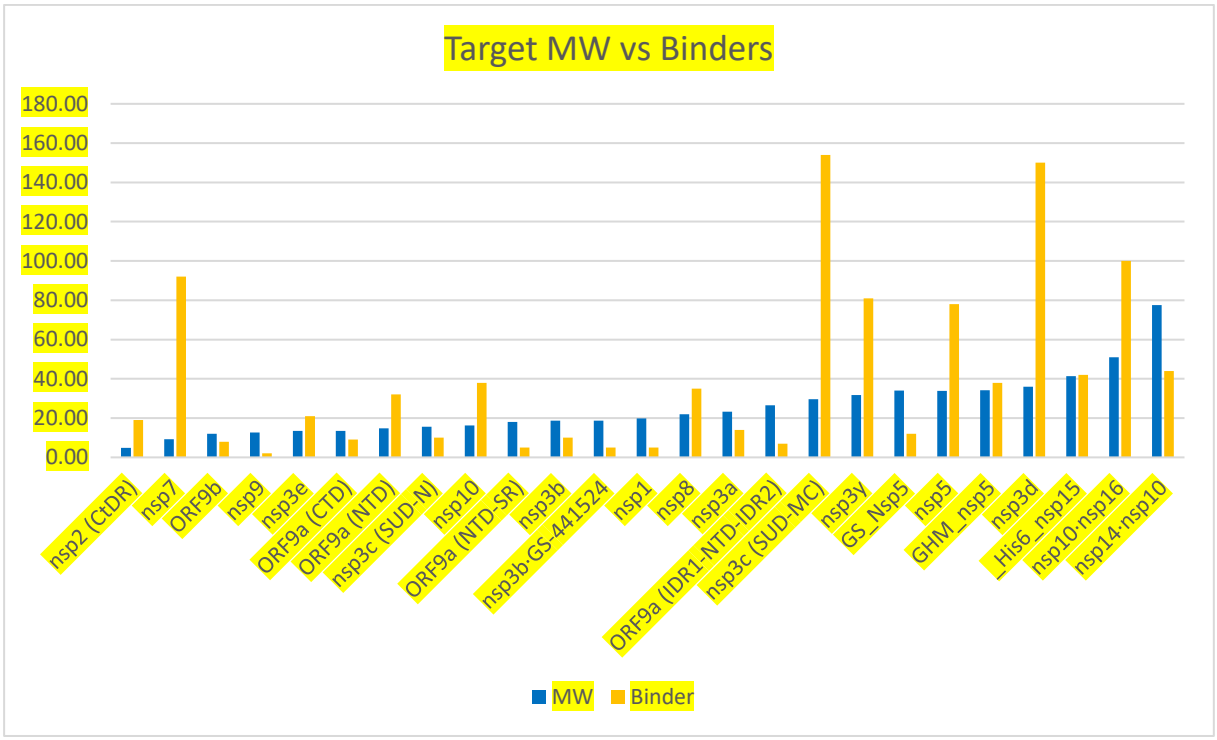

Supporting Information Figure 1: Number of binders and molecular weight of the screened protein constructs.

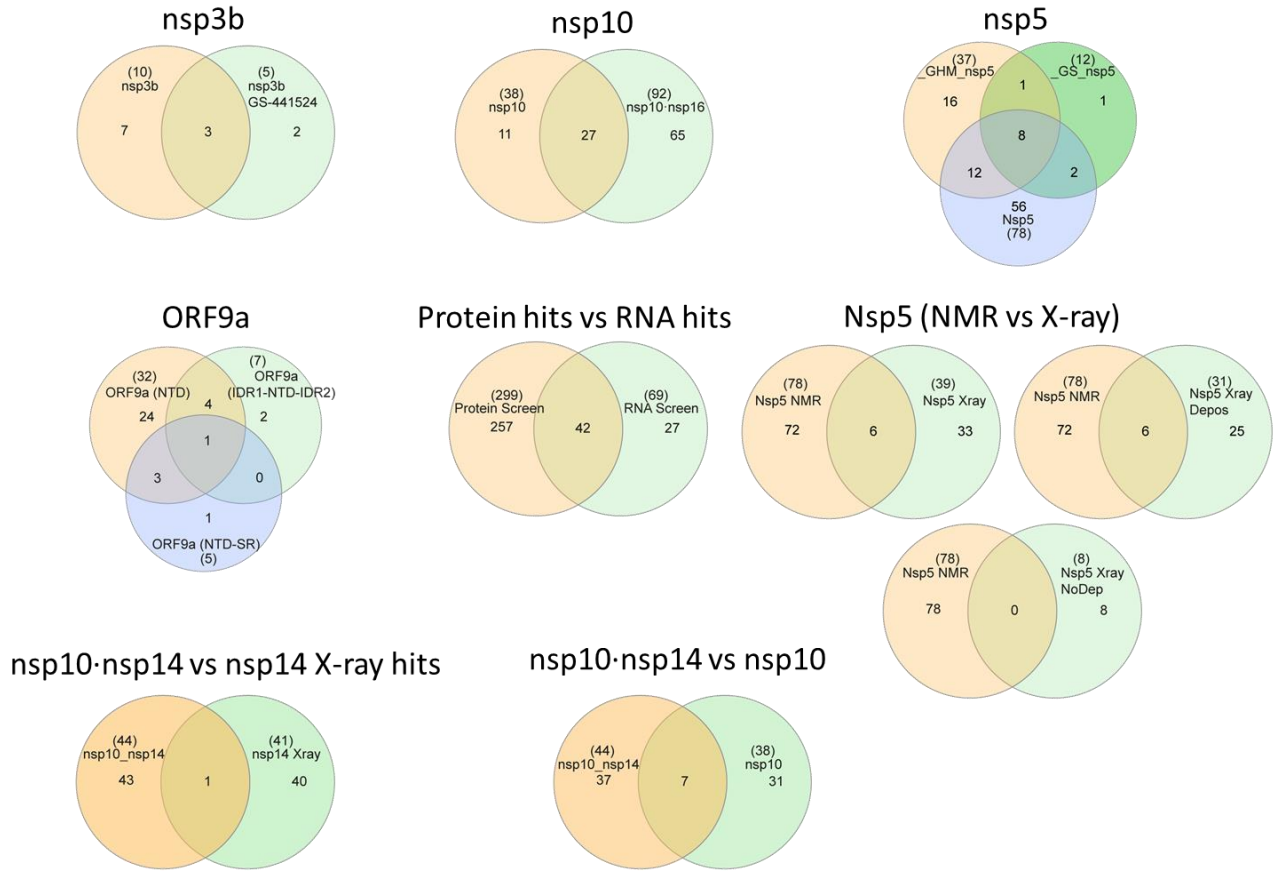

Supporting Information Figure 2: Venn diagrams of the binders of different sub-constructs of screened proteins.

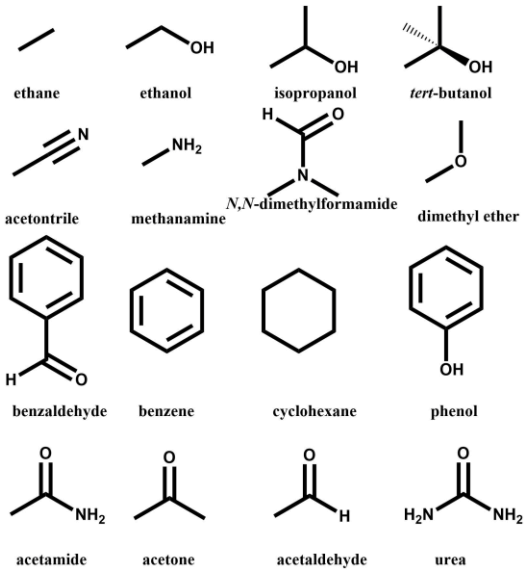

Supporting Information Figure 3: The 16 probes used in the analysation with FTMap.

nsp1 binders (manuscript number)
1
2
3
4
5

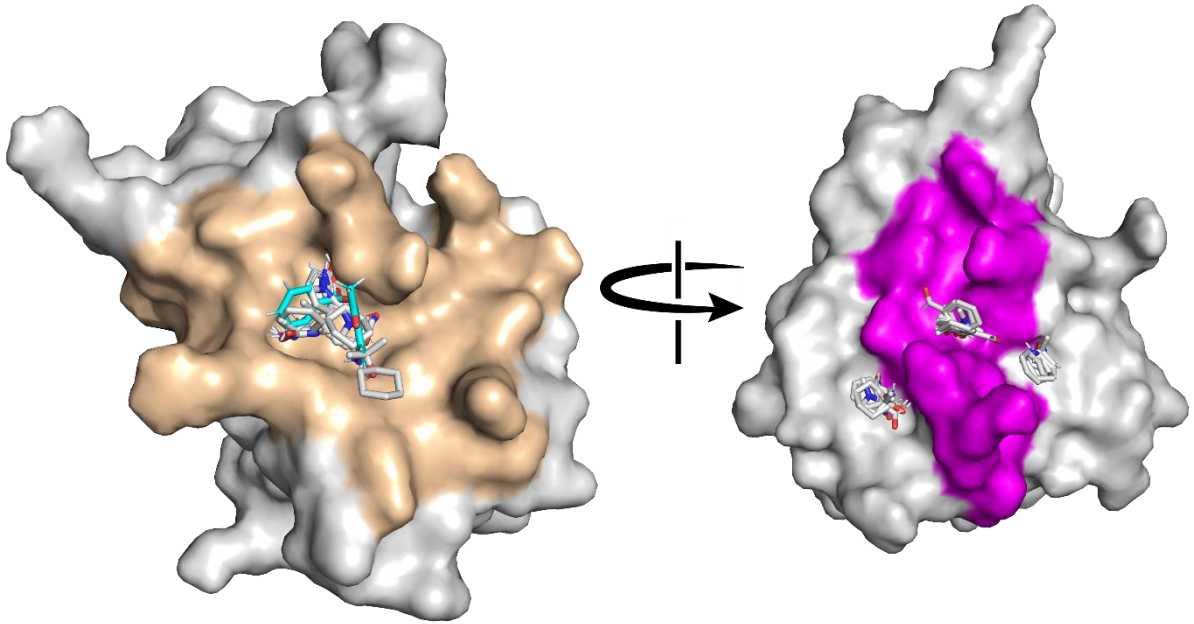

Supporting Information Figure 4: nsp1 (PDB: 7k7p) cleft 1 (beige) and 2 (magenta) with its corresponding cross clusters of FTMap probes (grey sticks) and the docked Binder 1 (cyan).

nsp3e binders (manuscript number)
39
40
41
42
43
44
45
46
47
48
49
50
51
52
53
54
55
56
57
58
59

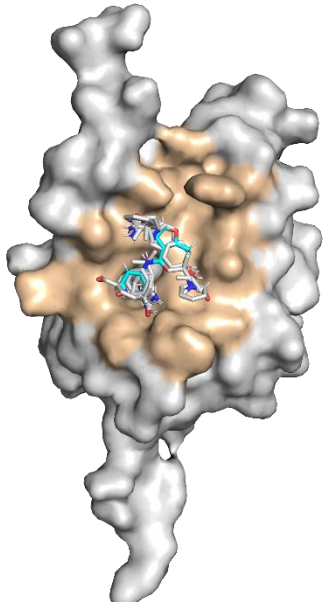

Supporting Information Figure 5: nsp3e (PDB: 2k87) cleft 3 (beige) with its corresponding cross clusters of FTMap probes (grey sticks) and the docked Binder 39 (cyan).

nsp3a binders (manuscript number)
3
60
61
62
31
33
4
5
1
2
63
52
64
32

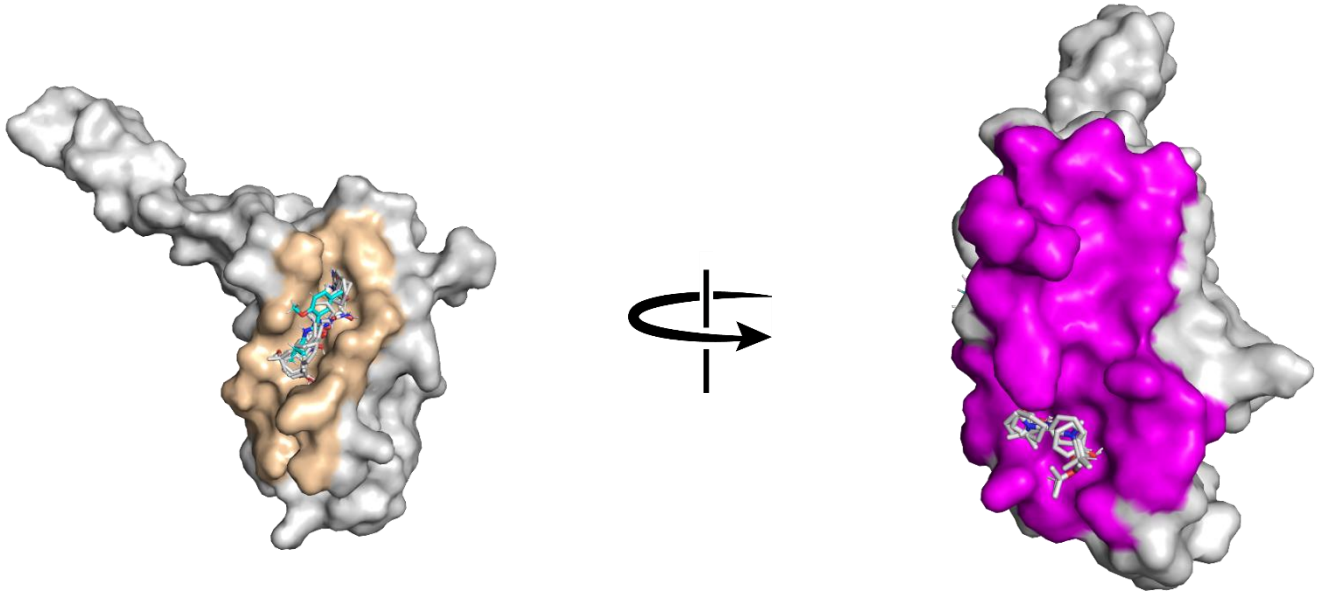

Supporting Information Figure 6: nsp3a (PDB: 7kag) cleft 2 (beige) and 1 (magenta) with its corresponding cross clusters of FTMap probes (grey sticks) and the docked Binder 61 (cyan).

nsp9 binders (manuscript number)
30
4

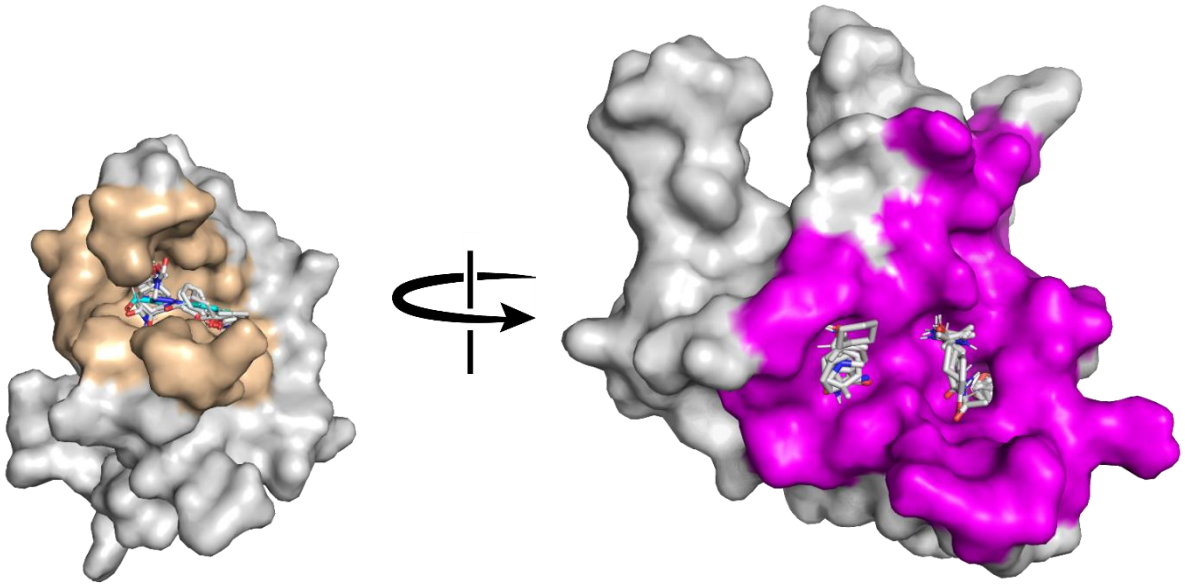

Supporting Information Figure 7: nsp9 (PDB: 6w4b) cleft 1 (beige) and 2 (magenta) with its corresponding cross clusters of FTMap probes (grey sticks) and the docked Binder 30 (cyan).

nsp7 (manuscript number)			binders
1	63	97	7
2	62	98	117
20	83	99	118
65	52	17	119
66	84	100	120
67	85	101	121
68	86	102	122
69	26	58	123
39	16	103	124
22	30	104	125
70	87	36	126
71	64	18	
9	31	38	
72	32	105	
73	88	106	
74	33	107	
75	4	108	
3	89	8	
60	90	109	
76	91	110	
61	92	28	
77	56	111	
78	5	112	
79	93	113	
80	94	114	
81	95	115	
82	96	116	

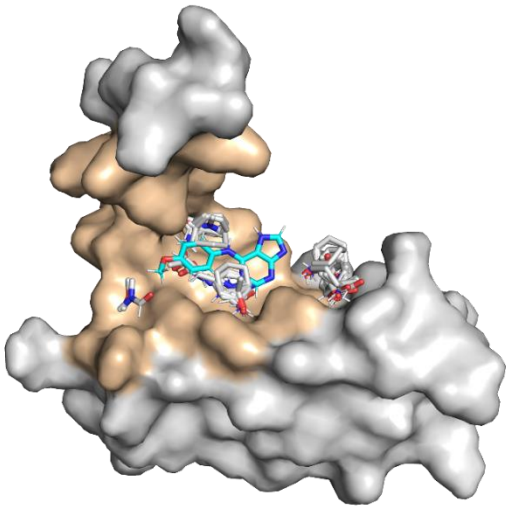

Supporting Information Figure 8: nsp7 (PDB: 6wiq) cleft 1 (beige) with its corresponding cross clusters of FTMap probes (grey sticks) and the docked Binder 65 (cyan).

nsp8 (manuscript number)	binders
127	131
75	30
62	33
112	55
1	117
2	132
3	57
60	121
31	99
32	
4	
5	
107	
91	
19	
20	
128	
65	
66	
108	
39	
129	
130	
72	
76	
61	

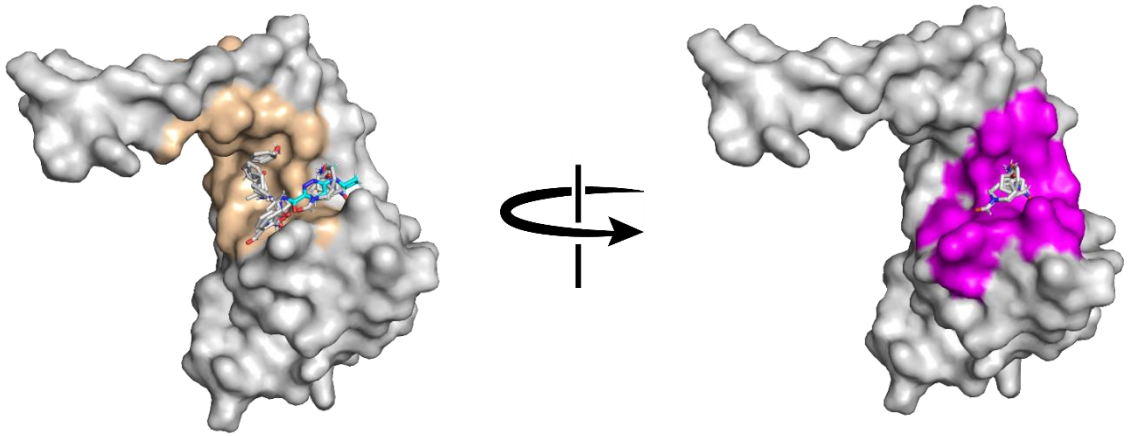

Supporting Information Figure 9: nsp8 (PDB: 6wiq) cleft 1 (beige) and 2 (magenta) with its corresponding cross clusters of FTMap probes (grey sticks) and the docked Binder 112 (cyan).

nsp3c (SUD-N) binders (manuscript number)
66
68
39
133
134
135
30
117
33

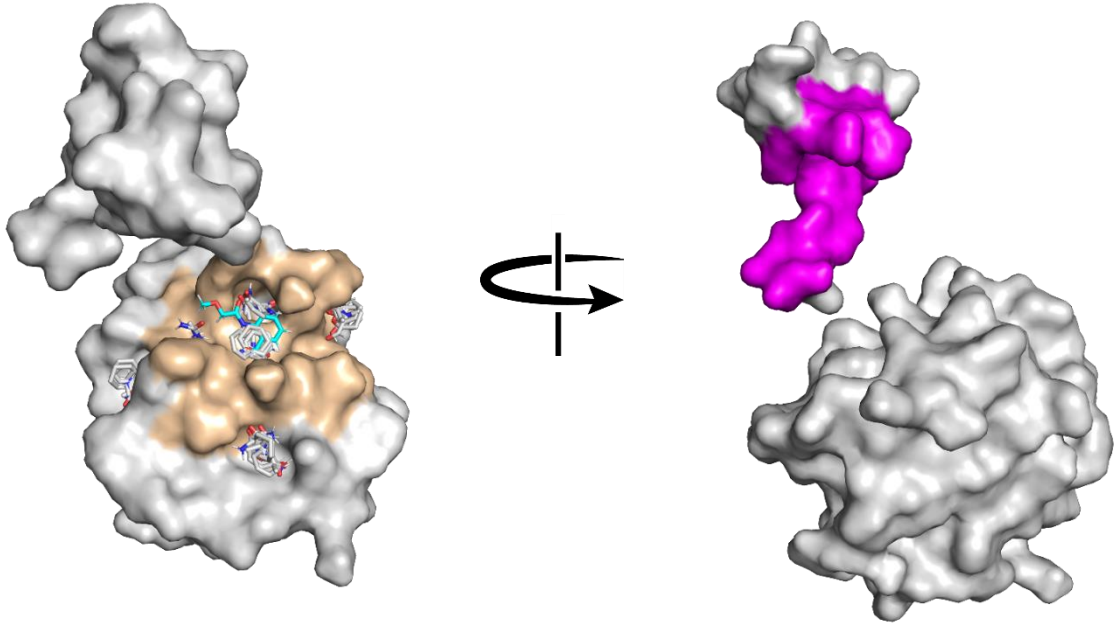

Supporting Information Figure 10: nsp3 (SUD-N) (PDB: 2w2g) cleft 1 (beige) and 2 (magenta) with its corresponding cross clusters of FTMap probes (grey sticks) and the docked Binder 134 (cyan).

nsp3c (SUD-MC) binders (manuscript number)					
67	152	169	84	117	18
68	153	74	85	56	38
30	39	170	86	192	124
4	21	11	179	120	200
66	22	13	26	5	201
80	154	171	16	93	202
136	129	172	180	193	203
1	70	173	181	94	204
2	155	174	182	95	127
137	156	75	87	96	106
138	41	3	183	98	205
20	71	175	112	99	206
139	157	60	31	194	119
128	158	76	32	17	207
140	159	61	184	123	69
65	160	109	185	100	168
141	161	48	113	101	178
142	9	49	114	102	92
143	10	131	186	58	199
144	162	78	187	59	
145	72	79	89	195	
146	163	176	188	196	
147	164	81	116	103	
148	165	177	90	104	
149	166	82	189	197	
150	167	62	190	36	
151	73	52	191	198	

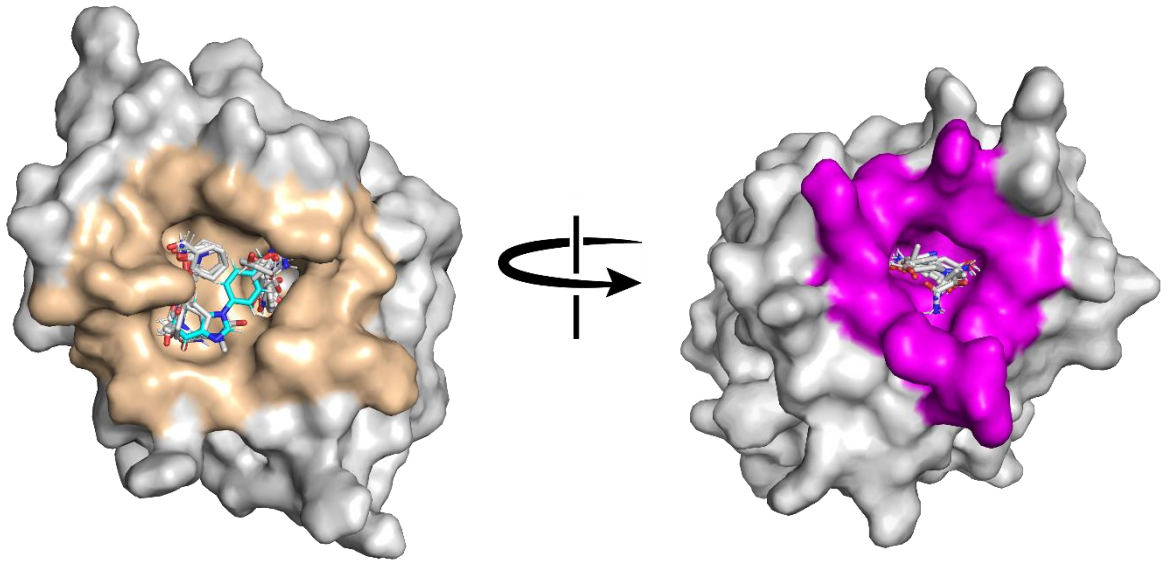

Supporting Information Figure 11: nsp3c (SUD-MC) (PDB: 2kqv) cleft 1 (beige) and 2 (magenta) with its corresponding cross clusters of FTMap probes (grey sticks) and the docked Binder 68 (cyan).

ORF9a (NTD) binders (manuscript number)	
55	28
66	111
108	4
72	56
47	38
134	213
208	
209	
206	
7	
118	
193	
132	
121	
210	
59	
128	
39	
22	
211	
129	
40	
41	
42	
212	
133	

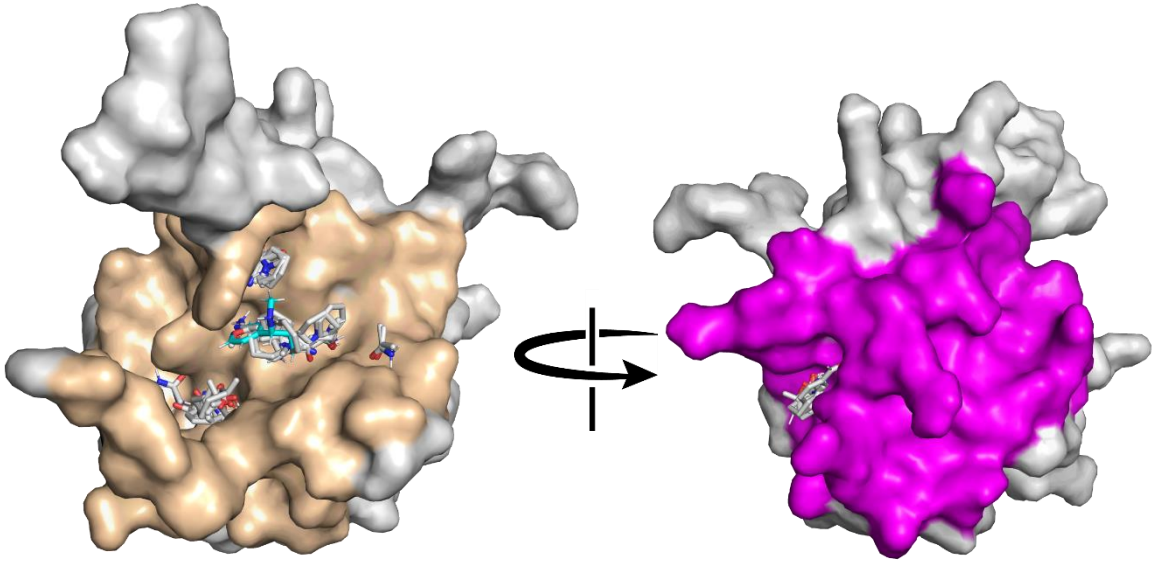

Supporting Information Figure 12: ORF9a (NTD) (PDB: 6yi3) cleft 1 (beige) and 2 (magenta) with its corresponding cross clusters of FTMap probes (grey sticks) and the docked Binder 55 (cyan).

nsp3b binders (manuscript number)
41
76
214

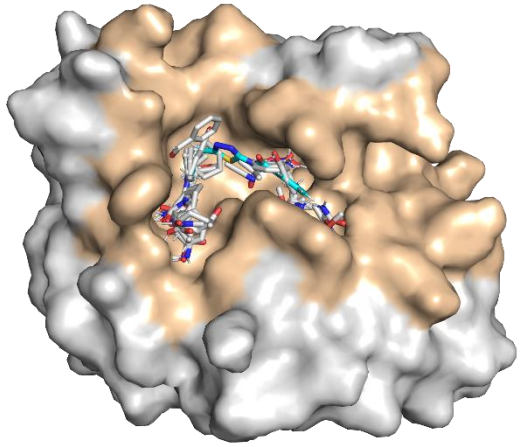

Supporting Information Figure 13: nsp3b (PDB: 6vxs) cleft 1 (beige) with its corresponding cross clusters of FTMap probes (grey sticks) and the docked Binder 41 (cyan).

nsp3d binders (manuscript number)					
1	167	178	92	124	189
128	73	84	117	126	259
217	225	205	192	202	260
65	168	86	120	203	261
66	226	181	240	127	207
141	227	233	5	106	262
145	45	234	241	146	263
152	74	111	93	67	264
218	228	214	242	68	147
153	133	209	243	211	36
39	229	182	193	249	199
219	230	30	94	250	
21	231	185	95	251	
22	172	235	96	252	
220	174	113	97	71	
156	75	4	99	253	
221	3	236	194	254	
157	60	114	244	255	
222	76	186	101	175	
223	109	187	245	61	
9	77	237	102	256	
10	232	89	246	257	
162	78	188	58	176	
72	81	116	59	51	
224	82	238	103	258	
163	63	90	247	6	
165	62	239	248	33	
166	52	191	38	115	

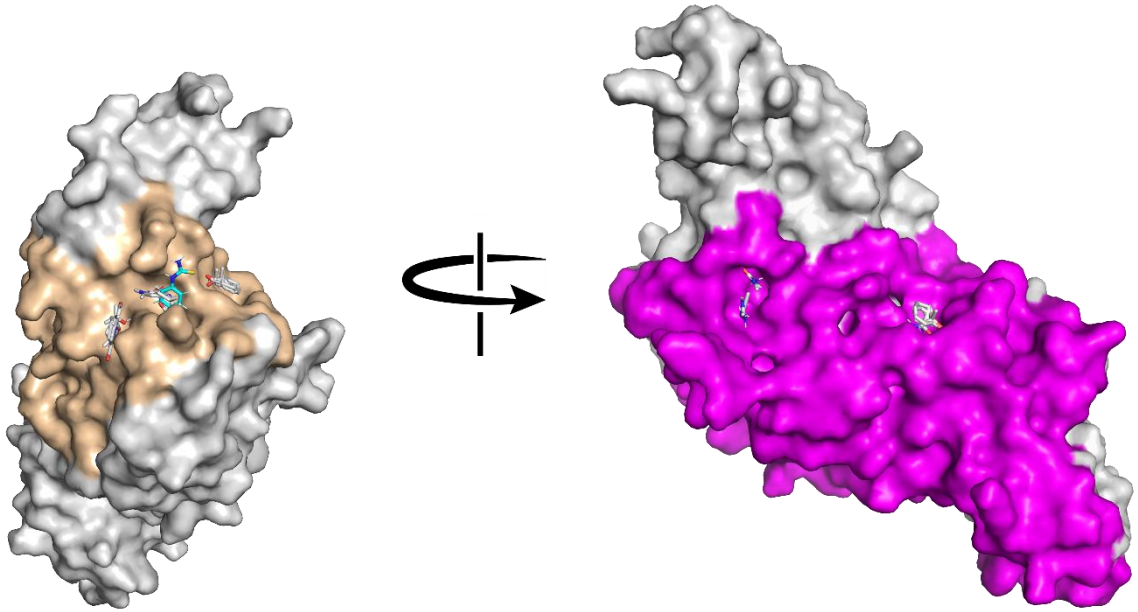

Supporting Information Figure 14: nsp3d (PDB: 6w9c) cleft 2 (beige) and 1 (magenta) with its corresponding cross clusters of FTMap probes (grey sticks) and the docked Binder 199 (cyan).

$_{His6}$nsp15 binders (manuscript number)	
33	208
115	233
107	265
2	111
21	113
22	5
3	98
32	210
4	65
186	81
91	266
36	82
1	52
31	16
20	62
143	258
108	
9	
72	
45	
74	
213	
60	
76	
48	
78	

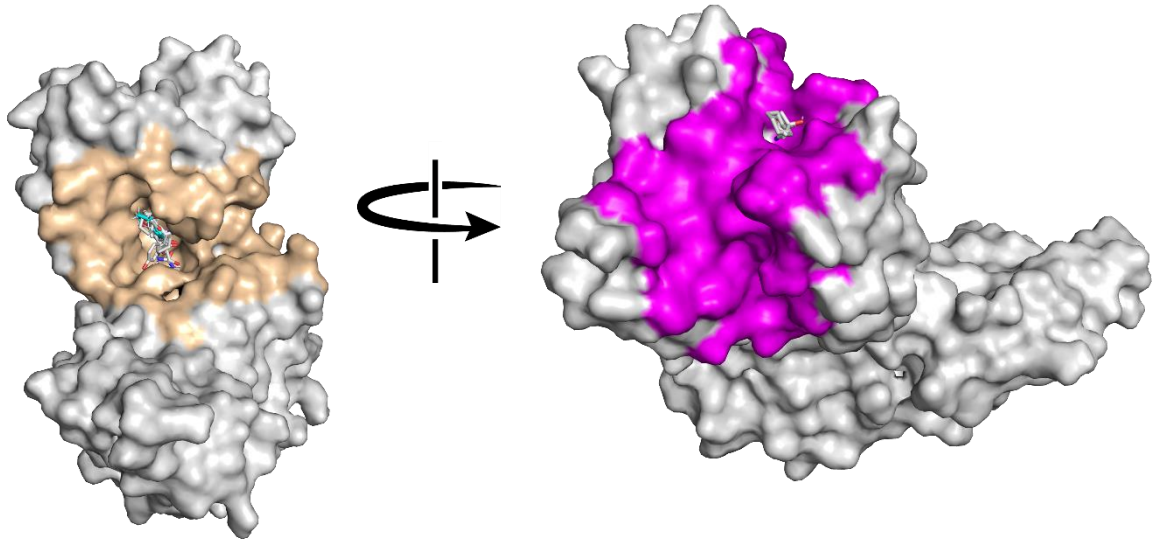

Supporting Information Figure 15: $_{His6}$nsp15 (PDB: 6w01) cleft 1 (beige) and 2 (magenta) with its corresponding cross clusters of FTMap probes (grey sticks) and the docked Binder 115 (cyan).

ORF9a (CTD) binders (manuscript number)
213
30
7
59
40
130
72
45
267

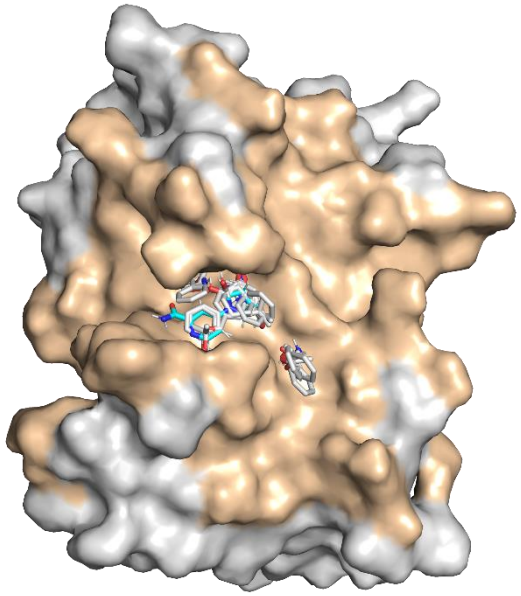

Supporting Information Figure 16: ORF9a (CTD) (PDB: 7c22) cleft 1 (beige) and 2 (magenta) with its corresponding cross clusters of FTMap probes (grey sticks) and the docked Binder 40 (cyan).

nsp10 binders (manuscript number)	
1	123
2	18
30	38
32	204
4	127
203	106
148	20
67	8
68	9
11	269
12	99
13	17
176	
80	
81	
16	
268	
87	
31	
113	
33	
91	
5	
97	
57	
121	

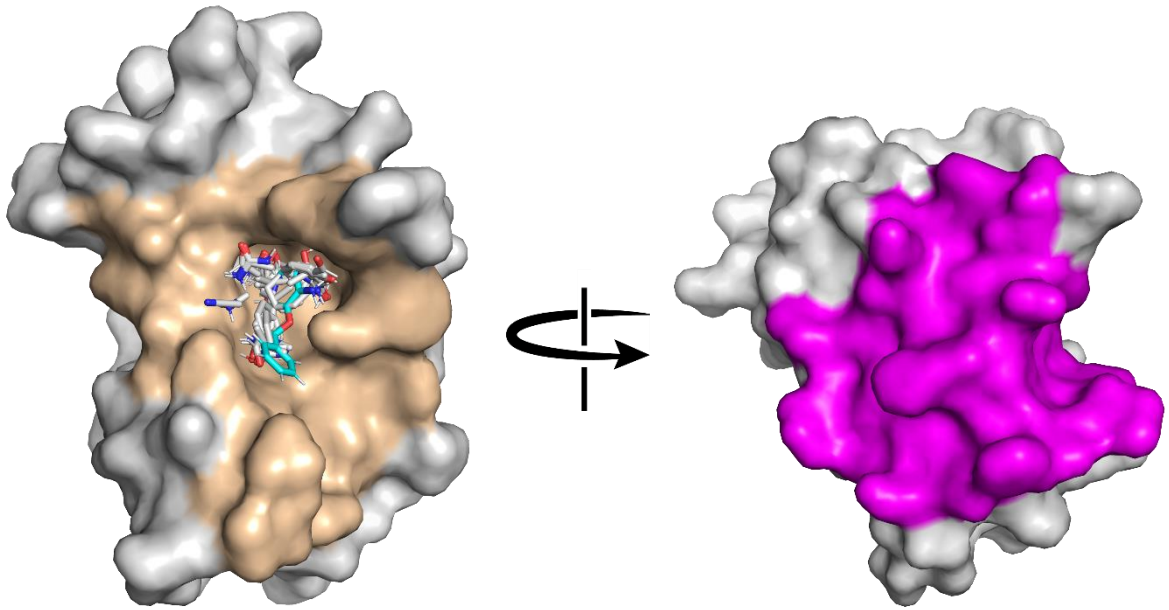

Supporting Information Figure 17: nsp10 (PDB: 6zpe) cleft 1 (beige) and 2 (magenta) with its corresponding cross clusters of FTMap probes (grey sticks) and the docked Binder 2 (cyan).

nsp10•nsp16 (manuscript number)			binders
1	170	184	199
276	271	113	18
273	274	88	37
2	11	33	38
137	12	4	124
19	13	89	200
20	75	90	202
139	3	239	203
140	60	91	204
65	61	92	127
66	109	117	106
145	270	5	107
67	78	94	311
149	80	96	167
68	81	98	23
152	63	99	76
218	62	17	84
153	52	101	275
39	26	245	193
21	16	246	
22	181	58	
220	30	196	
71	87	103	
9	272	104	
72	64	197	
73	31	36	
74	32	198	

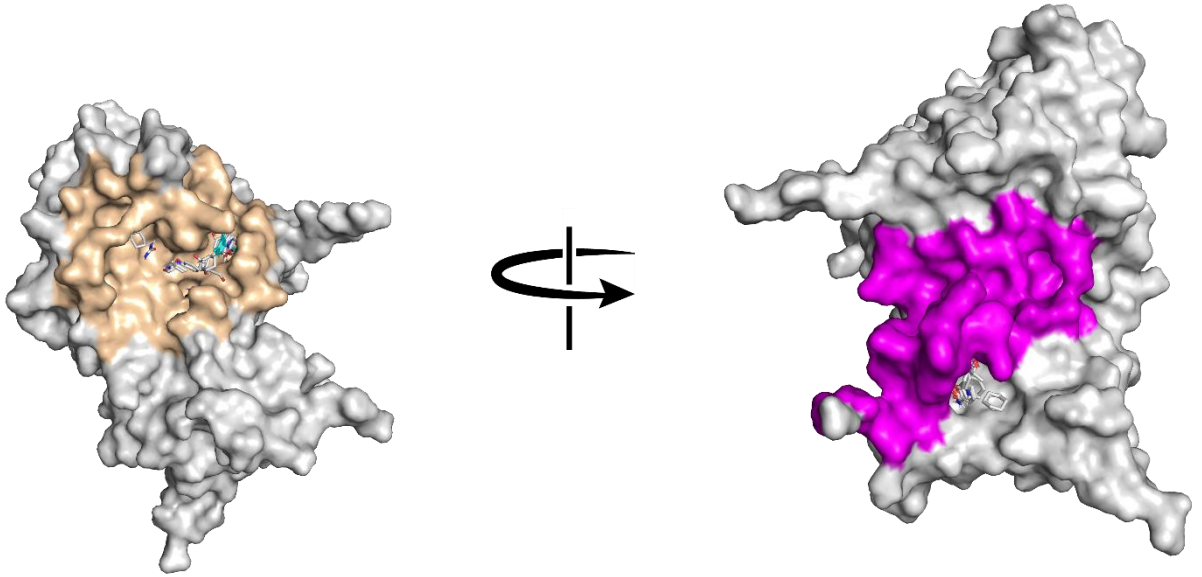

Supporting Information Figure 18: nsp10·nsp16 (PDB: 6w4h) cleft 1 (beige) and 2 (magenta) with its corresponding cross clusters of FTMap probes (grey sticks) and the docked Binder 4 (cyan).

ORF9b binders (manuscript number)
2
4
30
32
7
193
245
59

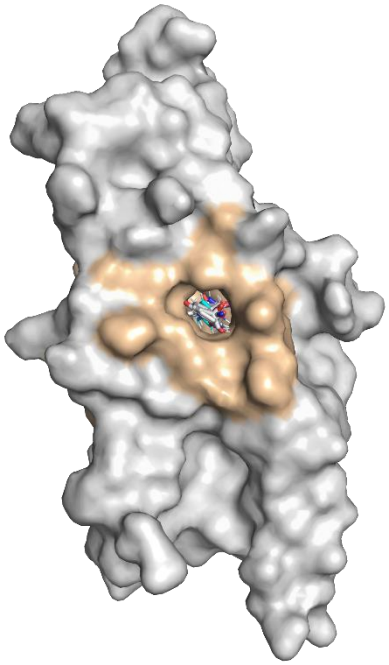

Supporting Information Figure 19: ORF9b (PDB: 6z4u) cleft 1 (beige) with its corresponding cross clusters of FTMap probes (grey sticks) and the docked Binder 2 (cyan).

nsp5 (manuscript number)	binders	
293	87	292
145	183	147
13	272	151
98	33	170
17	4	271
103	90	295
104	189	172
125	239	26
202	91	180
203	191	181
204	92	31
1	117	121
276	5	99
273	97	201
2	36	113
20	37	105
139	38	137
144	124	67
149	294	3
68	127	296
21	106	297
161	263	185
9	107	298
10	142	299
11	8	
12	16	
30	277	

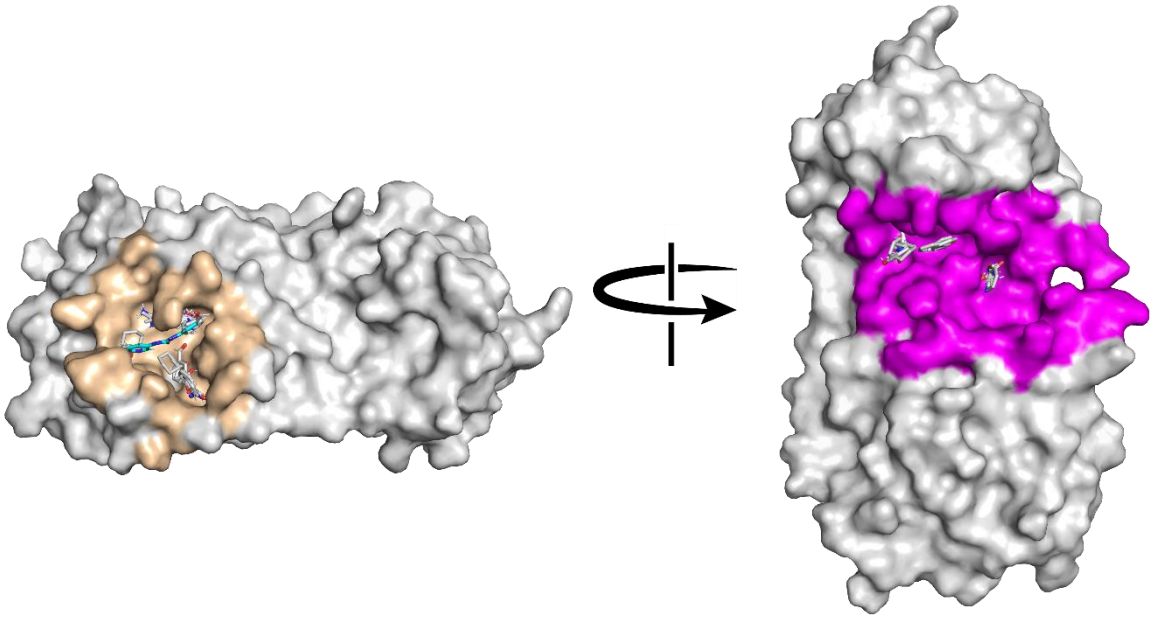

Supporting Information Figure 20: nsp5 (PDB: 6yb7) cleft 2 (beige) and 1 (magenta) with its corresponding cross clusters of FTMap probes (grey sticks) and the docked Binder 21 (cyan).

nsp10·nsp14 binders (manuscript number)	
3	165
11	168
16	194
18	199
19	222
21	229
26	300
32	301
39	302
58	303
59	304
61	305
66	306
67	307
86	308
91	309
98	310
99	
100	
114	
138	
141	
144	
145	
146	
149	
156	

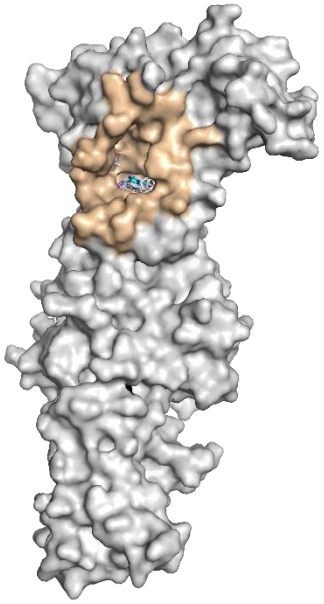

Supporting Information Figure 21: nsp10·nsp14 (PDB: nsp10·nsp14_modelled) cleft 3 (beige) with its corresponding cross clusters of FTMap probes (grey sticks) and the docked Binder 141 (cyan).

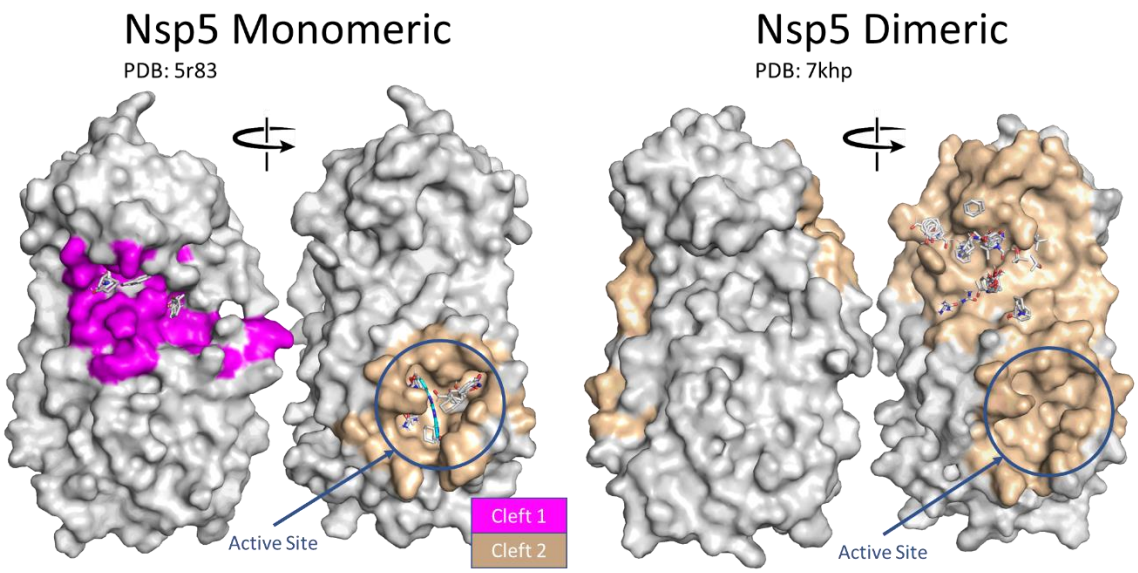

Supporting Information Figure 22: Difference in FTMap crossclusters when using a monomeric or dimeric version of nsp5 (second part of dimer not shown to be able to see the crossclusters in the dimeric interaction site).

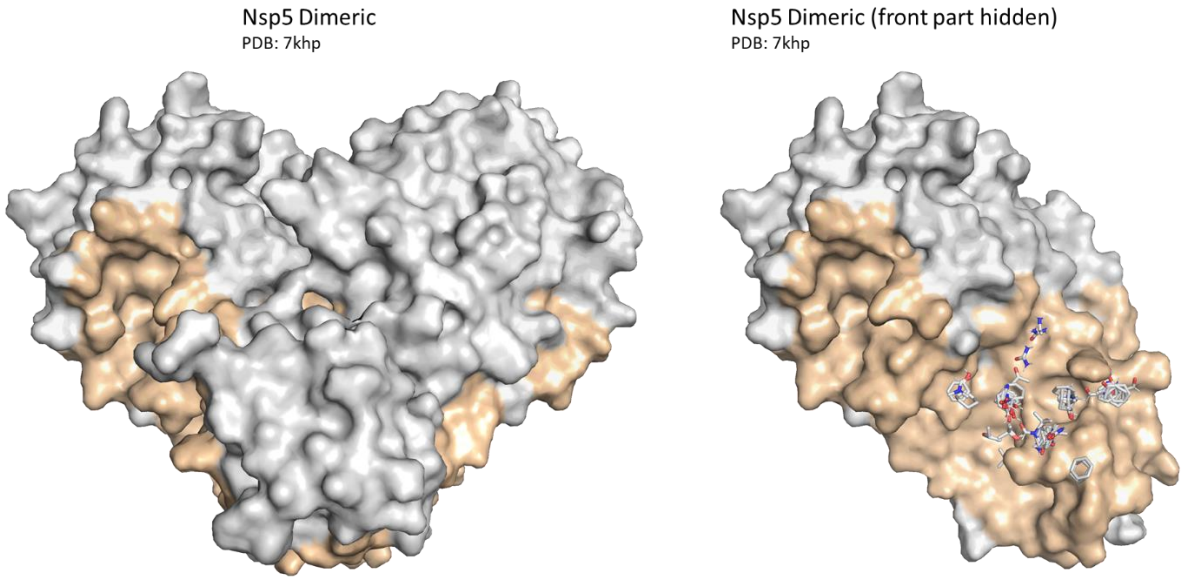

Supporting Information Figure 23: FTMap analysis run on the dimeric version of nsp5, with one part of the dimer hidden on the right side to show the underlying FTMap crossclusters.

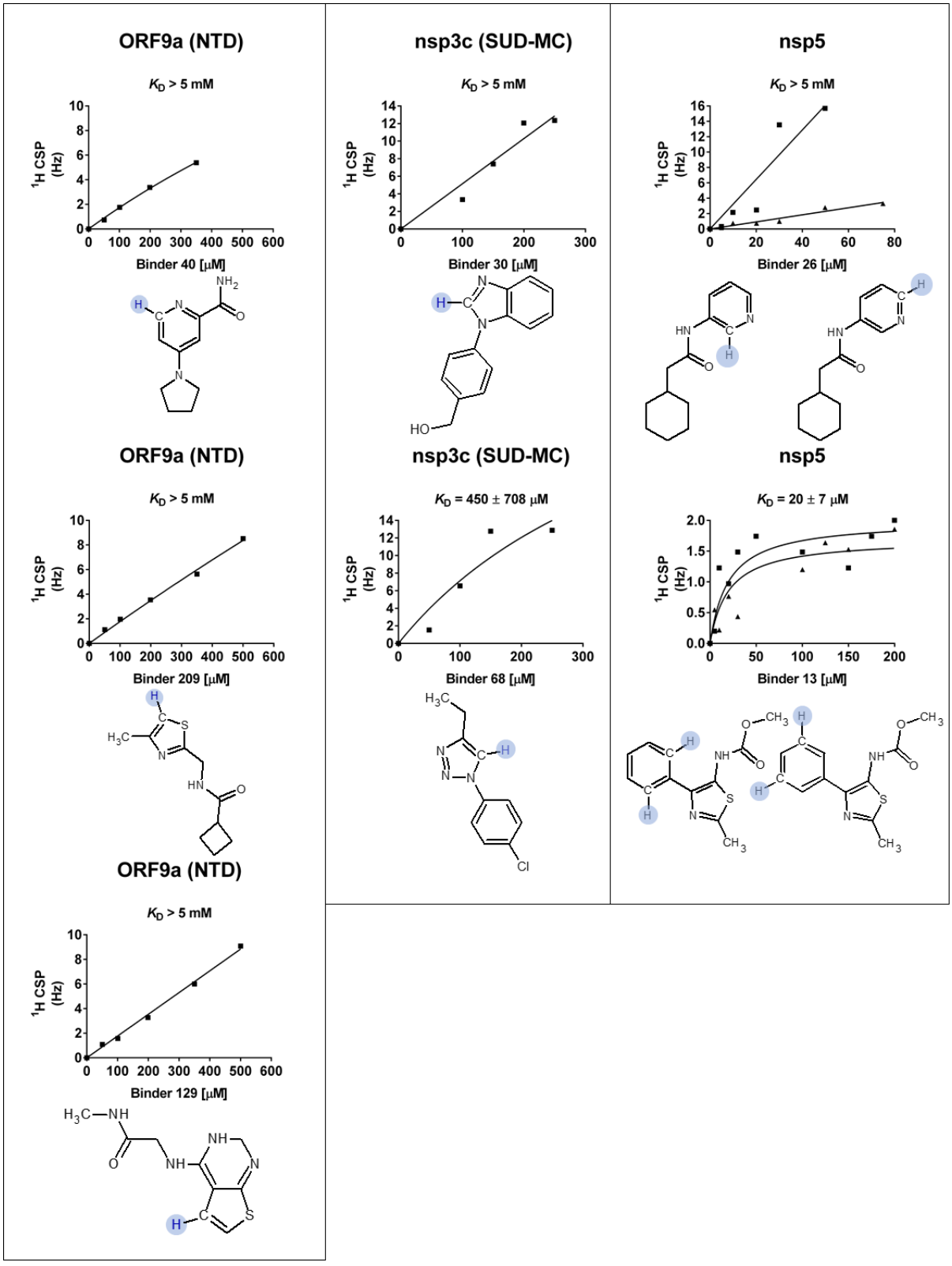

Supporting Information Figure 24: Ligand-observed titration for different binders with ORF9a (NTD), nsp3c (SUD-MC), and nsp5.

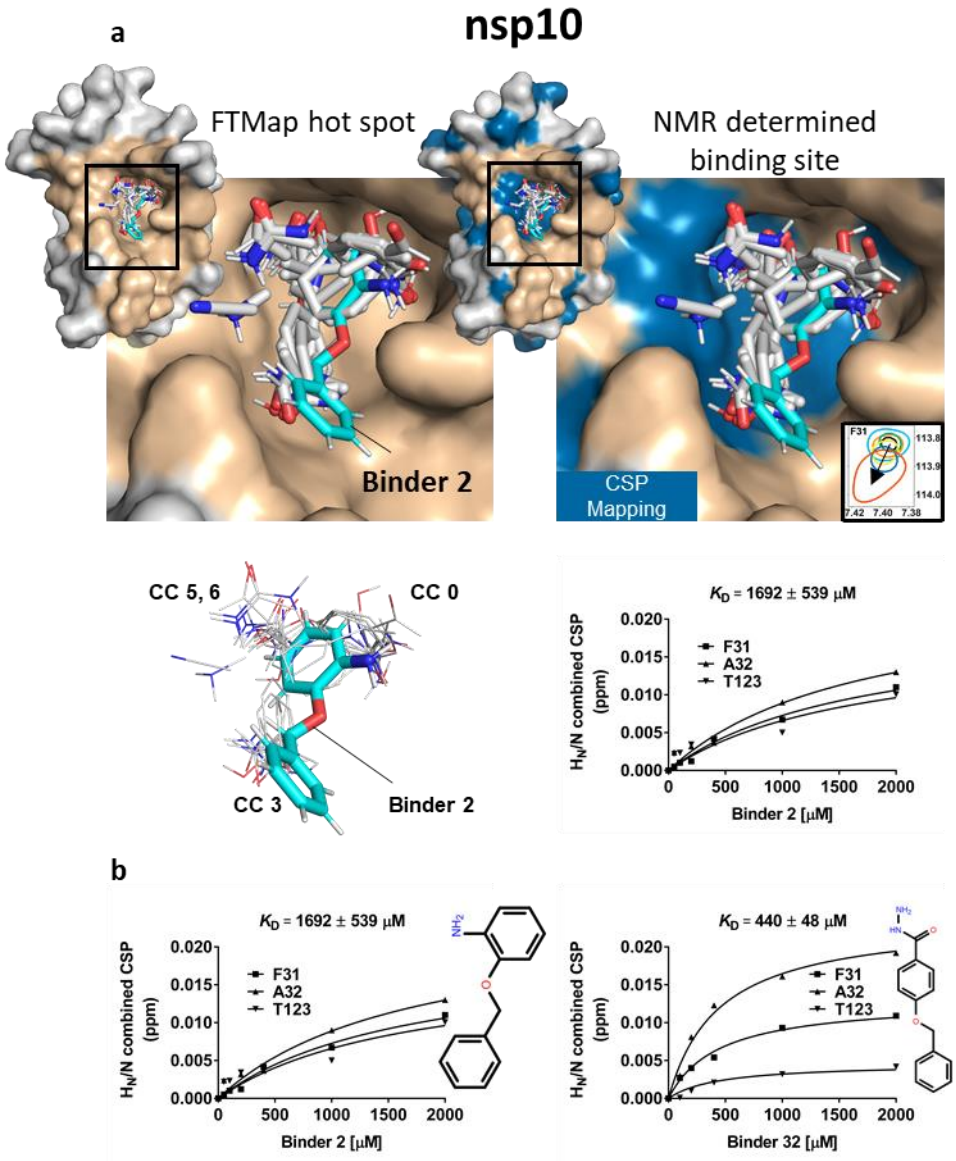

Supporting Information Figure 25: Protein observed titration of ligands with nsp10. a) left: binder 2 docked onto nsp10 with the FTMap hotspots around it. Right: binder 2 docked onto nsp10 with the FTMap hotspots around it and the amino acids with CSP's mapped in blue. Bottom left: Binder 2 with the indicated FTMap hotspots. Bottom right: Titration curve of binder 2 with nsp10. b) Titration curves of three different amino acids protein observed for binder 2 and binder 32.

A

Ligand	Docked to Monomer	Docked to Dimer
	found in active site (yes/no)	
144	no	yes
125	yes	yes
91	yes	yes
26	yes	yes
21	yes	yes
13	no	yes

B Ligand 21 0_0 pose in monomeric and dimeric nsp5 version

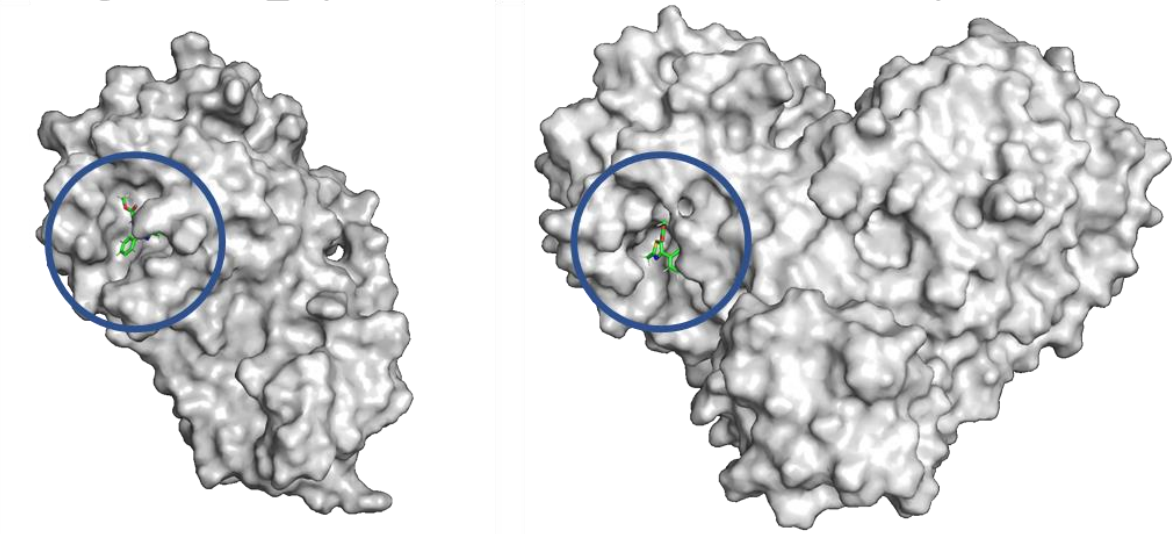

C Ligand 13 0_0 pose in monomeric and dimeric nsp5 version

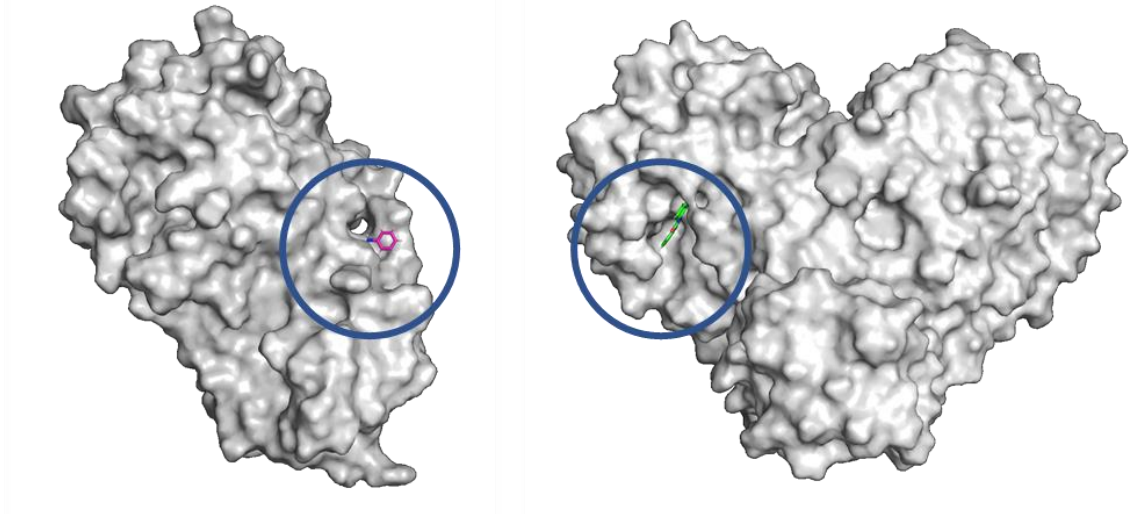

Supporting Information Figure 24Docking of the 6 overlapping X-ray/NMR binders to the monomeric and dimeric state of nsp5. (A) Table listing the docking results for 0_0 pose (energy minimum state). (B) Ligand 21 docks to the active site in both monomeric and dimeric nsp5. (C) Ligand 13 docks to the active site only in the dimeric state.

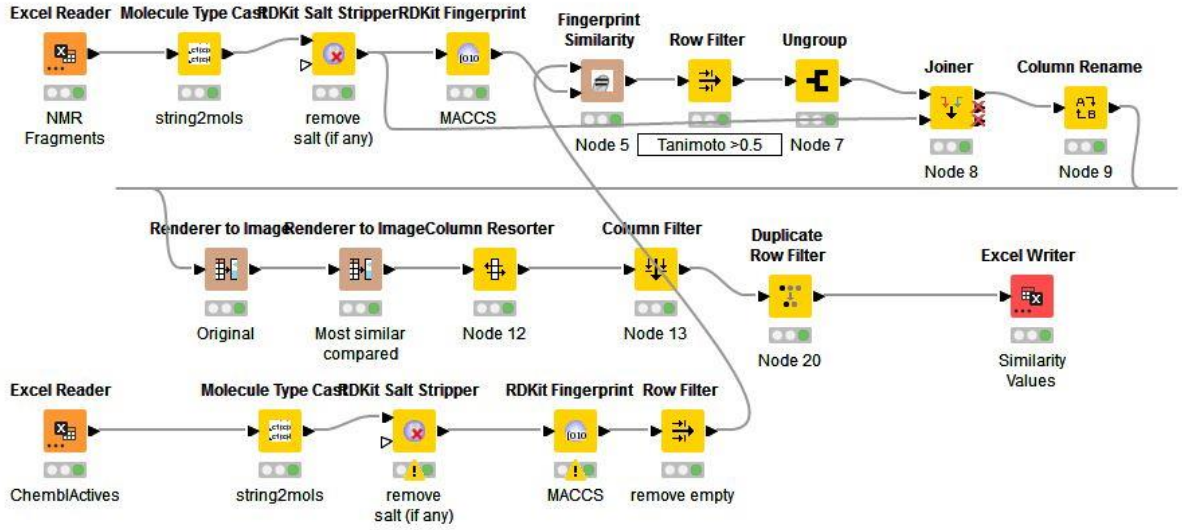

Supporting Information Figure 27: A snapshot of the KNIME workflow used for analog search. This workflow can be found at https://github.com/Fraunhofer-ITMP/KNIME_NMR

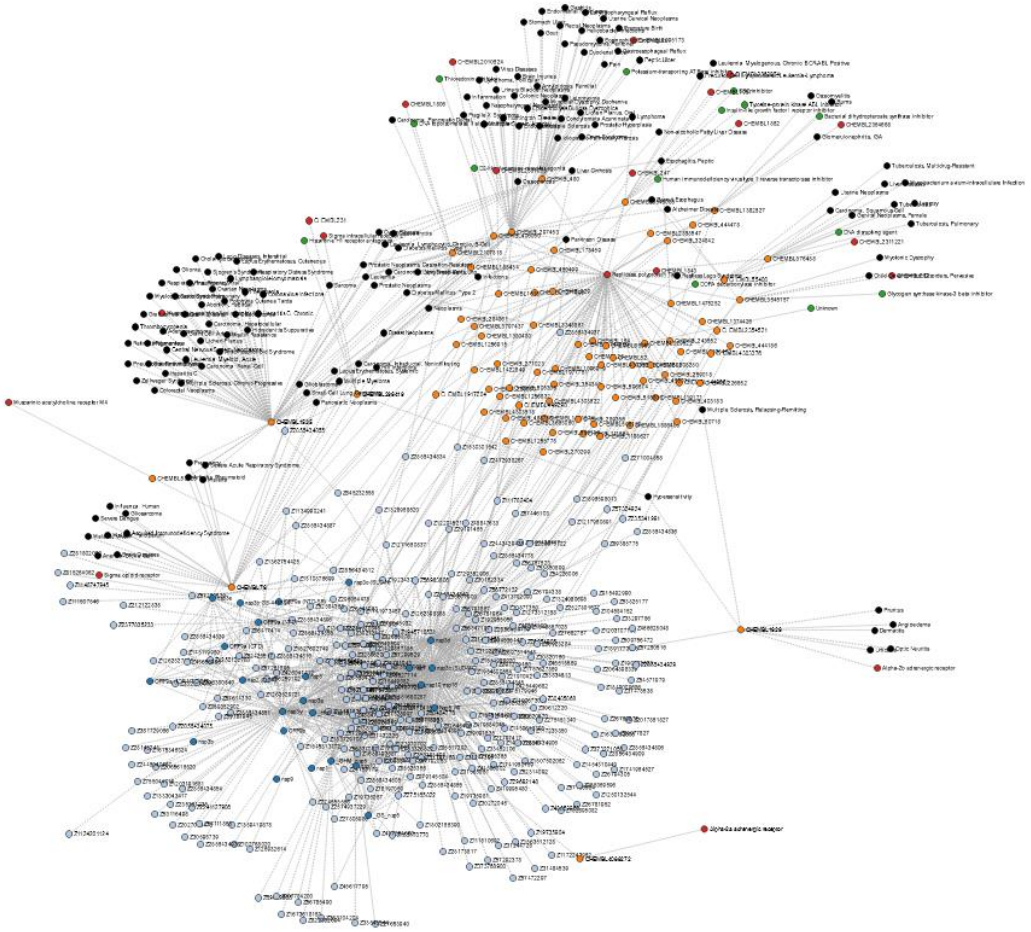

Supporting Information Figure 28: Knowledge graph embedding NMR data and results from SARS-CoV-2 bioactive analogues identified in the ChEMBL and PubChem databases. The codes written to generate the KG can be found at https://github.com/Fraunhofer-ITMP/COVID-NMR-KG. The KG is available for User navigation using the Cytoscape interface at the same location.

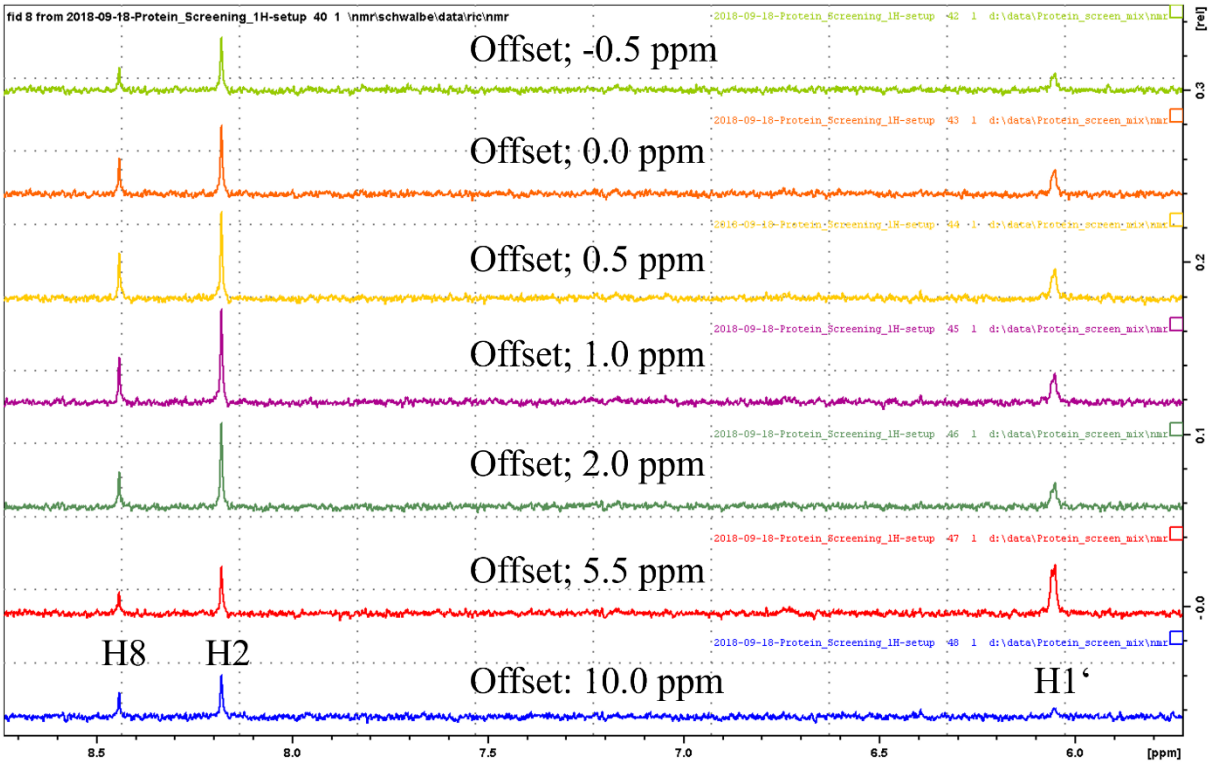

Supporting Information Figure 29: Optimization of NMR sequences and parameters for ligand-based NMR screening Optimization of STD parameters: Optimizing offset in the STD experiment. The optimization was done for a complex sample containing 1 mM AMP-PNP + 10 uM EPHA2 Kinase (34 kDa). The experiments were recorded at 600 MHz using 128 scans.

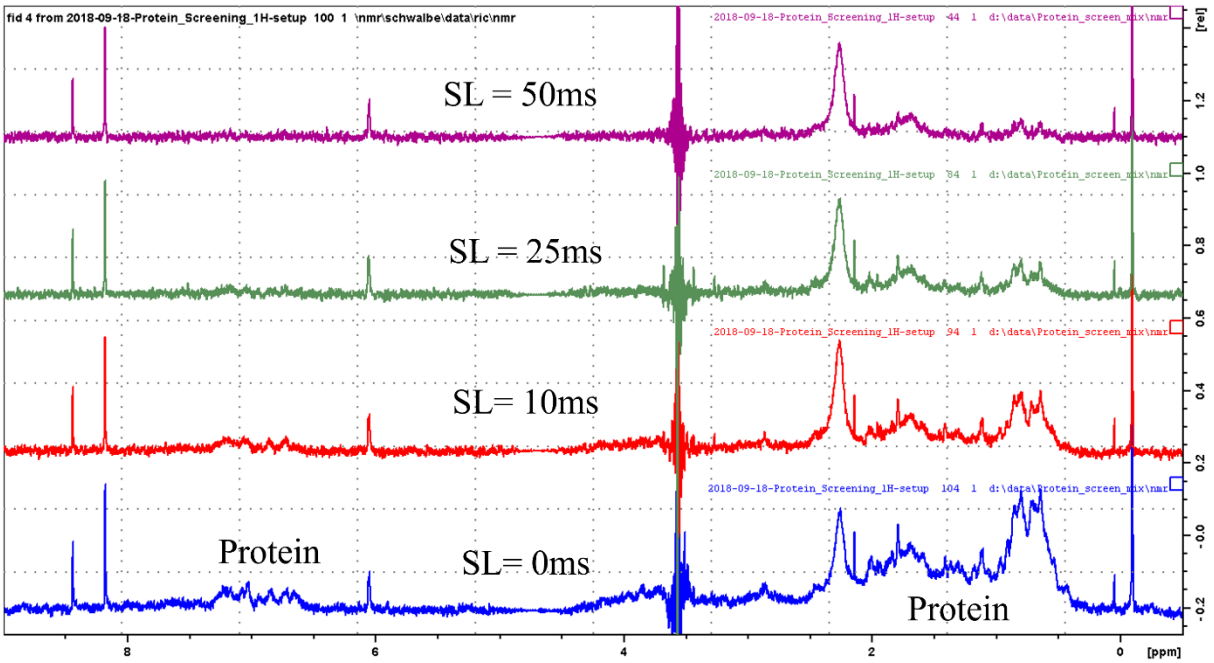

Supporting Information Figure 30: Optimization of NMR sequences and parameters for ligand-based NMR screening Optimization of STD parameters: Optimizing spin lock time in the STD experiment. The optimization was done for a complex sample containing 1 mM AMP-PNP + 10 uM EPHA2 Kinase (34 kDa). The experiments were recorded at 600 MHz using 128 scans.

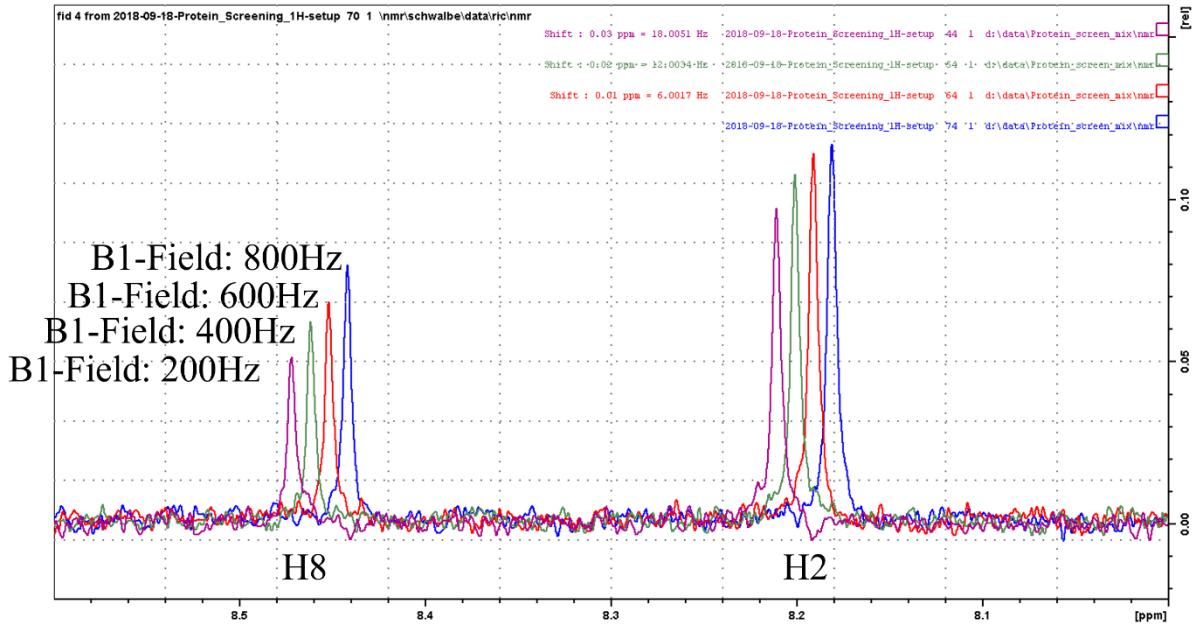

Supporting Information Figure 31: Optimization of NMR sequences and parameters for ligand-based NMR screening Optimization of STD parameters: Optimizing spin lock time in the STD experiment. The optimization was done for a complex sample containing 1 mM AMP-PNP + 10 uM EPHA2 Kinase (34 kDa). The experiments were recorded at 600 MHz using 128 scans.

Supporting Information Table 8: Proteins and their corresponding BMRBbig id's for the deposited excel files.

Protein	**BMRBbig id**
nsp1	bmrbig48
_GHM_nsp5	bmrbig45
nsp3e	bmrbig56
nsp3a	bmrbig50
nsp9	bmrbig61
nsp7	bmrbig59
nsp8	bmrbig60
nsp3c (SUD-N)	bmrbig54
nsp3c (SUD-MC)	bmrbig53
ORF9a (NTD)	bmrbig67
ORF9a (IDR1-NTD-IDR2)	bmrbig66
nsp3b	bmrbig51
nsp2 (CtDR)	bmrbig49
nsp3b·GS-441524	bmrbig52
nsp3d	bmrbig55
_His6_nsp15	bmrbig46
_GS_nsp5	bmrbig47
ORF9a (CTD)	bmrbig65
nsp10	bmrbig62
ORF9a (NTD-SR)	bmrbig68
nsp10·nsp16	bmrbig63
ORF9b	bmrbig69
nsp3y	bmrbig57
nsp5	bmrbig58
nsp10·nsp14	bmrbig64

References

[1] D. Adam, *Nature* **2022**, *601*, 312–315.

[2] G. J. Kontoghiorghes, S. Fetta, C. N. Kontoghiorghe, *Front Biosci (Landmark Ed)* **2021**, *26*, 1723–1736.

[3] Z. A. Shyr, K. Gorshkov, C. Z. Chen, W. Zheng, *Journal of Pharmacology and Experimental Therapeutics* **2020**, *375*, 127–138.

[4] T. T. Le, J. P. Cramer, R. Chen, S. Mayhew, *Evolution of the COVID-19 Vaccine Development Landscape*, Nature Reviews **2020,** *19*, 667-668.

[5] M. Mei, X. Tan, *Frontiers in Molecular Biosciences* **2021**, *8*, DOI 10.3389/fmolb.2021.671263.

[6] M. Cully, *Nature Reviews Drug Discovery* **2022**, *21*, 3–5.

[7] E. Petersen, F. Ntoumi, D. S. Hui, A. Abubakar, L. D. Kramer, C. Obiero, P. A. Tambyah, L. Blumberg, R. Yapi, S. Al-Abri, T. de C. A. Pinto, D. Yeboah-Manu, N. Haider, D. Asogun, T. P. Velavan, N. Kapata, M. Bates, R. Ansumana, C. Montaldo, L. Mucheleng'anga, J. Tembo, P. Mwaba, C. M. Himwaze, M. M. A. Hamid, S. Mfinanga, L. Mboera, T. Raj, E. Aklillu, F. Veas, S. Edwards, P. Kaleebu, T. D. McHugh, J. Chakaya, T. Nyirenda, M. Bockarie, P. S. Nyasulu, C. Wejse, J.-J. Muyembe-Tamfum, E. I. Azhar, M. Maeurer, J. B. Nachega, R. Kock, G. Ippolito, A. Zumla, *International Journal of Infectious Diseases* **2022**, *114*, 268–272.

[8] M. Hoffmann, N. Krüger, S. Schulz, A. Cossmann, C. Rocha, A. Kempf, I. Nehlmeier, L. Graichen, A.-S. Moldenhauer, M. S. Winkler, M. Lier, A. Dopfer-Jablonka, H.-M. Jäck, G. M. N. Behrens, S. Pöhlmann, *Cell* **2021**, *185*, 447-456, DOI 10.1016/j.cell.2021.12.032.

[9] L. A. VanBlargan, J. M. Errico, P. J. Halfmann, S. J. Zost, J. E. Crowe, L. A. Purcell, Y. Kawaoka, D. Corti, D. H. Fremont, M. S. Diamond, *Nature Medicine* **2022**, *28*, 490-495, DOI 10.1038/s41591-021-01678-y.

[10] W. F. Garcia-Beltran, K. J. st. Denis, A. Hoelzemer, E. C. Lam, A. D. Nitido, M. L. Sheehan, C. Berrios, O. Ofoman, C. C. Chang, B. M. Hauser, J. Feldman, A. L. Roederer, D. J. Gregory, M. C. Poznansky, A. G. Schmidt, A. J. Iafrate, V. Naranbhai, A. B. Balazs, *Cell* **2022**, *185*, 457-466, DOI 10.1016/j.cell.2021.12.033.

[11] Y.-W. Zhou, Y. Xie, L.-S. Tang, D. Pu, Y.-J. Zhu, J.-Y. Liu, X.-L. Ma, *Signal Transduction and Targeted Therapy* **2021**, *6*, 317.

[12] B. Malone, N. Urakova, E. J. Snijder, E. A. Campbell, *Nature Reviews Molecular Cell Biology* **2022**, *23*, 21–39.

[13] F. Wu, S. Zhao, B. Yu, Y.-M. Chen, W. Wang, Z.-G. Song, Y. Hu, Z.-W. Tao, J.-H. Tian, Y.-Y. Pei, M.-L. Yuan, Y.-L. Zhang, F.-H. Dai, Y. Liu, Q.-M. Wang, J.-J. Zheng, L. Xu, E. C. Holmes, Y.-Z. Zhang, *Nature* **2020**, *579*, 265–269.

[14] A. R. Fehr, S. Perlman, *Methods Mol Biol* **2015**, *1282*, 1–23.

[15] E. J. Snijder, P. J. Bredenbeek, J. C. Dobbe, V. Thiel, J. Ziebuhr, L. L. M. Poon, Y. Guan, M. Rozanov, W. J. M. Spaan, A. E. Gorbalenya, *J Mol Biol* **2003**, *331*, 991–1004.

[16] D. E. Gordon, G. M. Jang, M. Bouhaddou, J. Xu, K. Obernier, K. M. White, M. J. O'Meara, V. v. Rezelj, J. Z. Guo, D. L. Swaney, T. A. Tummino, R. Hüttenhain, R. M. Kaake, A. L. Richards, B. Tutuncuoglu, H. Foussard, J. Batra, K. Haas, M. Modak, M. Kim, P. Haas, B. J. Polacco, H. Braberg, J. M. Fabius, M. Eckhardt, M. Soucheray, M. J. Bennett, M. Cakir, M. J. McGregor, Q. Li, B. Meyer, F. Roesch, T. Vallet, A. mac Kain, L. Miorin, E. Moreno, Z. Z. C. Naing, Y. Zhou, S. Peng, Y. Shi, Z. Zhang, W. Shen, I. T. Kirby, J. E. Melnyk, J. S. Chorba, K. Lou, S. A. Dai, I. Barrio-Hernandez, D. Memon, C. Hernandez-Armenta, J. Lyu, C. J. P. Mathy, T. Perica, K. B. Pilla, S. J. Ganesan, D. J. Saltzberg, R. Rakesh, X. Liu, S. B. Rosenthal, L. Calviello, S. Venkataramanan, J. Liboy-Lugo, Y. Lin, X. P. Huang, Y. F. Liu, S. A. Wankowicz, M. Bohn, M. Safari, F. S. Ugur, C. Koh, N. S. Savar, Q. D. Tran, D. Shengjuler, S. J. Fletcher, M. C. O'Neal, Y. Cai, J. C. J. Chang, D. J. Broadhurst, S. Klippsten, P. P. Sharp, N. A. Wenzell, D. Kuzuoglu-Ozturk, H. Y. Wang, R. Trenker, J. M. Young, D. A. Cavero, J. Hiatt, T. L. Roth, U. Rathore, A. Subramanian, J. Noack, M. Hubert, R. M. Stroud, A. D. Frankel, O. S. Rosenberg, K. A. Verba, D. A. Agard, M. Ott, M. Emerman, N. Jura, M. von Zastrow, E. Verdin, A. Ashworth, O. Schwartz, C. d'Enfert, S. Mukherjee, M. Jacobson, H. S. Malik, D. G. Fujimori, T. Ideker, C. S. Craik, S. N. Floor, J. S. Fraser, J. D. Gross, A. Sali, B. L. Roth, D. Ruggero, J. Taunton, T. Kortemme, P. Beltrao, M. Vignuzzi, A. García-Sastre, K. M. Shokat, B. K. Shoichet, N. J. Krogan, *Nature* **2020**, *583*, 459–468.

[17] C. W. Nelson, Z. Ardern, T. L. Goldberg, C. Meng, C. H. Kuo, C. Ludwig, S. O. Kolokotronis, X. Wei, *Elife* **2020**, *9*, e59633.

[18] A. Pavesi, *Virology* **2020**, *546*, 51–66.

[19] P. Venkatesan, *The Lancet Respiratory Medicine* **2021**, *9*, e63.

[20] B. Cao, Y. Wang, D. Wen, W. Liu, J. Wang, G. Fan, L. Ruan, B. Song, Y. Cai, M. Wei, X. Li, J. Xia, N. Chen, J. Xiang, T. Yu, T. Bai, X. Xie, L. Zhang, C. Li, Y. Yuan, H. Chen, H. Li, H. Huang, S. Tu, F. Gong, Y. Liu, Y. Wei, C. Dong, F. Zhou, X. Gu, J. Xu, Z. Liu, Y. Zhang, H. Li, L. Shang, K. Wang, K. Li, X. Zhou, X. Dong, Z. Qu, S. Lu, X. Hu, S. Ruan, S. Luo, J. Wu, L. Peng, F. Cheng, L. Pan, J. Zou, C. Jia, J. Wang, X. Liu, S. Wang, X. Wu, Q. Ge, J. He, H. Zhan, F. Qiu, L. Guo, C. Huang, T. Jaki, F. G. Hayden, P. W. Horby, D. Zhang, C. Wang, *New England Journal of Medicine* **2020**, *382*, 1787–1799.

[21] M. Wang, R. Cao, L. Zhang, X. Yang, J. Liu, M. Xu, Z. Shi, Z. Hu, W. Zhong, G. Xiao, *Cell Research* **2020**, *30*, 269–271.

[22] W.-C. Ko, J.-M. Rolain, N.-Y. Lee, P.-L. Chen, C.-T. Huang, P.-I. Lee, P.-R. Hsueh, *International Journal of Antimicrobial Agents* **2020**, *55*, 105933.

[23] M. A. Martinez, *Frontiers in Immunology* **2021**, *12*, DOI 10.3389/fimmu.2021.635371.

[24] J. O. Ogidigo, E. A. Iwuchukwu, C. U. Ibeji, O. Okpalefe, M. E. S. Soliman, *Journal of Biomolecular Structure and Dynamics* **2020**, *40*, 2284–2301.

[25] C. Liu, X. Zhu, Y. Lu, X. Zhang, X. Jia, T. Yang, *Journal of Pharmaceutical Analysis* **2021**, *11*, 272–277.

[26] M. A. White, W. Lin, X. Cheng, *The Journal of Physical Chemistry Letters* **2020**, *11*, 9144–9151.

[27] M. T. J. Quimque, K. I. R. Notarte, R. A. T. Fernandez, M. A. O. Mendoza, R. A. D. Liman, J. A. K. Lim, L. A. E. Pilapil, J. K. H. Ong, A. M. Pastrana, A. Khan, D.-Q. Wei, A. P. G. Macabeo, *Journal of Biomolecular Structure and Dynamics* **2021**, *39*, 4316–4333.

[28] A. Carino, F. Moraca, B. Fiorillo, S. Marchianò, V. Sepe, M. Biagioli, C. Finamore, S. Bozza, D. Francisci, E. Distrutti, B. Catalanotti, A. Zampella, S. Fiorucci, *Frontiers in Chemistry* **2020**, *8*, DOI 10.3389/fchem.2020.572885.

[29] S. Barage, A. Karthic, R. Bavi, N. Desai, R. Kumar, V. Kumar, K. W. Lee, *Journal of Biomolecular Structure and Dynamics* **2020**, *40*, 2557-2574.

[30] M. Macchiagodena, M. Pagliai, P. Procacci, *Chemical Physics Letters* **2020**, *750*, 137489.

[31] S. Yazdani, N. de Maio, Y. Ding, V. Shahani, N. Goldman, M. Schapira, *Journal of Proteome Research* **2021**, *20*, 4212–4215.

[32] L. Zhang, D. Lin, X. Sun, U. Curth, C. Drosten, L. Sauerhering, S. Becker, K. Rox, R. Hilgenfeld, *Science (1979)* **2020**, *368*, 409–412.

[33] M. Schuller, G. J. Correy, S. Gahbauer, D. Fearon, T. Wu, R. E. Díaz, I. D. Young, L. Carvalho Martins, D. H. Smith, U. Schulze-Gahmen, T. W. Owens, I. Deshpande, G. E. Merz, A. C. Thwin, J. T. Biel, J. K. Peters, M. Moritz, N. Herrera, H. T. Kratochvil, A. Aimon, J. M. Bennett, J. Brandao Neto, A. E. Cohen, A. Dias, A. Douangamath, L. Dunnett, O. Fedorov, M. P. Ferla, M. R. Fuchs, T. J. Gorrie-Stone, J. M. Holton, M. G. Johnson, T. Krojer, G. Meigs, A. J. Powell, J. G. M. Rack, V. L. Rangel, S. Russi, R. E. Skyner, C. A. Smith, A. S. Soares, J. L. Wierman, K. Zhu, P. O'Brien, N. Jura, A. Ashworth, J. J. Irwin, M. C. Thompson, J. E. Gestwicki, F. von Delft, B. K. Shoichet, J. S. Fraser, I. Ahel, *Science Advances* **2021**, *7*, eabf8711, DOI 10.1126/sciadv.abf8711.

[34] S. Günther, P. Y. A. Reinke, Y. Fernández-García, J. Lieske, T. J. Lane, H. M. Ginn, F. H. M. Koua, C. Ehrt, W. Ewert, D. Oberthuer, O. Yefanov, S. Meier, K. Lorenzen, B. Krichel, J.-D. Kopicki, L. Gelisio, W. Brehm, I. Dunkel, B. Seychell, H. Gieseler, B. Norton-Baker, B. Escudero-Pérez, M. Domaracky, S. Saouane, A. Tolstikova, T. A. White, A. Hänle, M. Groessler, H. Fleckenstein, F. Trost, M. Galchenkova, Y. Gevorkov, C. Li, S. Awel, A. Peck, M. Barthelmess, F. Schlünzen, P. Lourdu Xavier, N. Werner, H. Andaleeb, N. Ullah, S. Falke, V. Srinivasan, B. A. França, M. Schwinzer, H. Brognaro, C. Rogers, D. Melo, J. J. Zaitseva-Doyle, J. Knoska, G. E. Peña-Murillo, A. R. Mashhour, V. Hennicke, P. Fischer, J. Hakanpää, J. Meyer, P. Gribbon, B. Ellinger, M. Kuzikov, M. Wolf, A. R. Beccari, G. Bourenkov, D. von Stetten, G. Pompidor, I. Bento, S. Panneerselvam, I. Karpics, T. R. Schneider, M. M. Garcia-Alai, S. Niebling, C. Günther, C. Schmidt, R. Schubert, H. Han, J. Boger, D. C. F. Monteiro, L. Zhang, X. Sun, J. Pletzer-Zelgert, J. Wollenhaupt, C. G. Feiler, M. S. Weiss, E.-C. Schulz, P. Mehrabi, K. Karničar, A. Usenik, J. Loboda, H. Tidow, A. Chari, R. Hilgenfeld, C. Uetrecht, R. Cox, A. Zaliani, T. Beck, M. Rarey, S. Günther, D. Turk, W. Hinrichs, H. N. Chapman, A. R. Pearson, C. Betzel, A. Meents, *Science (1979)* **2021**, *372*, 642–646.

[35] J. A. Newman, A. Douangamath, S. Yadzani, Y. Yosaatmadja, A. Aimon, J. Brandão-Neto, L. Dunnett, T. Gorrie-stone, R. Skyner, D. Fearon, M. Schapira, F. von Delft, O. Gileadi, *Nature Communications* **2021**, *12*, 4848.

[36] F. Cantrelle, E. Boll, L. Brier, D. Moschidi, S. Belouzard, V. Landry, F. Leroux, F. Dewitte, I. Landrieu, J. Dubuisson, B. Deprez, J. Charton, X. Hanoulle, *Angewandte Chemie International Edition* **2021**, *60*, 25428–25435.

[37] A. L. Kantsadi, E. Cattermole, M.-T. Matsoukas, G. A. Spyroulias, I. Vakonakis, *Journal of Biomolecular NMR* **2021**, *75*, 167–178.

[38] N. Imprachim, Y. Yosaatmadja, J. A. Newman, *bioRxiv* **2022**, 2022.03.11.483836.

[39] V. Napolitano, A. Dabrowska, K. Schorpp, A. Mourão, E. Barreto-Duran, M. Benedyk, P. Botwina, S. Brandner, M. Bostock, Y. Chykunova, A. Czarna, G. Dubin, T. Fröhlich, M. Hölscher, M. Jedrysik, A. Matsuda, K. Owczarek, M. Pachota, O. Plettenburg, J. Potempa, I. Rothenaigner, F. Schlauderer, K. Slysz, A. Szczepanski, K. Greve-Isdahl Mohn, B. Blomberg, M. Sattler, K. Hadian, G. M. Popowicz, K. Pyrc, *Cell Chemical Biology* **2022**, *29*, 774-784, DOI 10.1016/j.chembiol.2021.11.006.

[40] T. C. M. Consortium, H. Achdout, A. Aimon, E. Bar-David, H. Barr, A. Ben-Shmuel, J. Bennett, V. A. Bilenko, V. A. Bilenko, M. L. Boby, B. Borden, G. R. Bowman, J. Brun, S. BVNBS, M. Calmiano, A. Carbery, D. Carney, E. Cattermole, E. Chang, E. Chernyshenko, J. D. Chodera, A. Clyde, J. E. Coffland, G. Cohen, J. Cole, A. Contini, L. Cox, M. Cvitkovic, A. Dias, K. Donckers, D. L. Dotson, A. Douangamath, S. Duberstein, T. Dudgeon, L. Dunnett, P. K. Eastman, N. Erez, C. J. Eyermann, M. Fairhead, G. Fate, D. Fearon, O. Fedorov, M. Ferla, R. S. Fernandes, L. Ferrins, R. Foster, H. Foster, R. Gabizon, A. Garcia-Sastre, V. O. Gawriljuk, P. Gehrtz, C. Gileadi, C. Giroud, W. G. Glass, R. Glen, I. Glinert, A. S. Godoy, M. Gorichko, T. Gorrie-Stone, E. J. Griffen, S. H. Hart, J. Heer, M. Henry, M. Hill, S. Horrell, V. D. Huliak, M. F. D. Hurley, T. Israely, A. Jajack, J. Jansen, E. Jnoff, D. Jochmans, T. John, S. de Jonghe, A. L. Kantsadi, P. W. Kenny, J. L. Kiappes, S. O. Kinakh, L. Koekemoer, B. Kovar, T. Krojer, A. Lee, B. A. Lefker, H. Levy, I. G. Logvinenko, N. London, P. Lukacik, H. B. Macdonald, B. MacLean, T. R. Malla, T. Matviiuk, W. McCorkindale, B. L. McGovern, S. Melamed, K. P. Melnykov, O. Michurin, H. Mikolajek, B. F. Milne, A. Morris, G. M. Morris, M. J. Morwitzer, D. Moustakas, A. M. Nakamura, J. B. Neto, J. Neyts, L. Nguyen, G. D. Noske, V. Oleinikovas, G. Oliva, G. J. Overheul, D. Owen, R. Pai, J. Pan, N. Paran, B. Perry, M. Pingle, J. Pinjari, B. Politi, A. Powell, V. Psenak, R. Puni, V. L. Rangel, R. N. Reddi, S. P. Reid, E. Resnick, E. G. Ripka, M. C. Robinson, R. P. Robinson, J. Rodriguez-Guerra, R. Rosales, D. Rufa, K. Saar, K. S. Saikatendu, C. Schofield, M. Shafeev, A. Shaikh, J. Shi, K. Shurrush, S. Singh, A. Sittner, R. Skyner, A. Smalley, B. Smeets, M. D. Smilova, L. J. Solmesky, J. Spencer, C. Strain-Damerell, V. Swamy, H. Tamir, R. Tennant, W. Thompson, A. Thompson, S. Tomasio, I. S. Tsurupa, A. Tumber, I. Vakonakis, R. P. van Rij, L. Vangeel, F. S. Varghese, M. Vaschetto, E. B. Vitner, V. Voelz, A. Volkamer, F. von Delft, A. von Delft, M. Walsh, W. Ward, C. Weatherall, S. Weiss, K. M. White, C. F. Wild, M. Wittmann, N. Wright, Y. Yahalom-Ronen, D. Zaidmann, H. Zidane, N. Zitzmann, *bioRxiv* **2022**, 2020.10.29.339317.

[41] M. Kozlov, *Nature* **2022**, *601*, 496, DOI 10.1038/d41586-022-00112-8.

[42] J. F. X. Diffley, *Biochemical Journal* **2021**, *478*, 2533–2535.

[43] C. T. Lim, K. W. Tan, M. Wu, R. Ulferts, L. A. Armstrong, E. Ozono, L. S. Drury, J. C. Milligan, T. U. Zeisner, J. Zeng, F. Weissmann, B. Canal, G. Bineva-Todd, M. Howell, N. O'Reilly, R. Beale, Y. Kulathu, K. Labib, J. F. X. Diffley, *Biochemical Journal* **2021**, *478*, 2517–2531.

[44] J. C. Milligan, T. U. Zeisner, G. Papageorgiou, D. Joshi, C. Soudy, R. Ulferts, M. Wu, C. T. Lim, K. W. Tan, F. Weissmann, B. Canal, R. Fujisawa, T. Deegan, H. Nagaraj, G. Bineva-Todd, C. Basier, J. F. Curran, M. Howell, R. Beale, K. Labib, N. O'Reilly, J. F. X. Diffley, *Biochemical Journal* **2021**, *478*, 2499–2515.

[45] S. Basu, T. Mak, R. Ulferts, M. Wu, T. Deegan, R. Fujisawa, K. W. Tan, C. T. Lim, C. Basier, B. Canal, J. F. Curran, L. S. Drury, A. W. McClure, E. L. Roberts, F. Weissmann, T. U. Zeisner, R. Beale, V. H. Cowling, M. Howell, K. Labib, J. F. X. Diffley, *Biochemical Journal* **2021**, *478*, 2481–2497.

[46] B. Canal, R. Fujisawa, A. W. McClure, T. D. Deegan, M. Wu, R. Ulferts, F. Weissmann, L. S. Drury, A. P. Bertolin, J. Zeng, R. Beale, M. Howell, K. Labib, J. F. X. Diffley, *Biochemical Journal* **2021**, *478*, 2465–2479.

[47] B. Canal, A. W. McClure, J. F. Curran, M. Wu, R. Ulferts, F. Weissmann, J. Zeng, A. P. Bertolin, J. C. Milligan, S. Basu, L. S. Drury, T. D. Deegan, R. Fujisawa, E. L. Roberts, C. Basier, K. Labib, R. Beale, M. Howell, J. F. X. Diffley, *Biochemical Journal* **2021**, *478*, 2445–2464.

[48] A. P. Bertolin, F. Weissmann, J. Zeng, V. Posse, J. C. Milligan, B. Canal, R. Ulferts, M. Wu, L. S. Drury, M. Howell, R. Beale, J. F. X. Diffley, *Biochemical Journal* **2021**, *478*, 2425–2443.

[49] J. Zeng, F. Weissmann, A. P. Bertolin, V. Posse, B. Canal, R. Ulferts, M. Wu, R. Harvey, S. Hussain, J. C. Milligan, C. Roustan, A. Borg, L. McCoy, L. S. Drury, S. Kjaer, J. McCauley, M. Howell, R. Beale, J. F. X. Diffley, *Biochemical Journal* **2021**, *478*, 2405–2423.

[50] P. Ren, W. Shang, W. Yin, H. Ge, L. Wang, X. Zhang, B. Li, H. Li, Y. Xu, E. H. Xu, H. Jiang, L. Zhu, L. Zhang, F. Bai, *Acta Pharmacologica Sinica* **2022**, *43*, 483–493.

[51] N. Altincekic, S. M. Korn, N. S. Qureshi, M. Dujardin, M. Ninot-Pedrosa, R. Abele, M. J. Abi Saad, C. Alfano, F. C. L. Almeida, I. Alshamleh, G. C. de Amorim, T. K. Anderson, C. D. Anobom, C. Anorma, J. K. Bains, A. Bax, M. Blackledge, J. Blechar, A. Böckmann, L. Brigandat, A. Bula, M. Bütikofer, A. R. Camacho-Zarco, T. Carlomagno, I. P. Caruso, B. Ceylan, A. Chaikuad, F. Chu, L. Cole, M. G. Crosby, V. de Jesus, K. Dhamotharan, I. C. Felli, J. Ferner, Y. Fleischmann, M. L. Fogeron, N. K. Fourkiotis, C. Fuks, B. Fürtig, A. Gallo, S. L. Gande, J. A. Gerez, D. Ghosh, F. Gomes-Neto, O. Gorbatyuk, S. Guseva, C. Hacker, S. Häfner, B. Hao, B. Hargittay, K. Henzler-Wildman, J. C. Hoch, K. F. Hohmann, M. T. Hutchison, K. Jaudzems, K. Jović, J. Kaderli, G. Kalniņš, I. Kaņepe, R. N. Kirchdoerfer, J. Kirkpatrick, S. Knapp, R. Krishnathas, F. Kutz, S. zur Lage, R. Lambertz, A. Lang, D. Laurents, L. Lecoq, V. Linhard, F. Löhr, A. Malki, L. M. Bessa, R. W. Martin, T. Matzel, D. Maurin, S. W. McNutt, N. C. Mebus-Antunes, B. H. Meier, N. Meiser, M. Mompeán, E. Monaca, R. Montserret, L. Mariño Perez, C. Moser, C. Muhle-Goll, T. C. Neves-Martins, X. Ni, B. Norton-Baker, R. Pierattelli, L. Pontoriero, Y. Pustovalova, O. Ohlenschläger, J. Orts, A. T. da Poian, D. J. Pyper, C. Richter, R. Riek, C. M. Rienstra, A. Robertson, A. S. Pinheiro, R. Sabbatella, N. Salvi, K. Saxena, L. Schulte, M. Schiavina, H. Schwalbe, M. Silber, M. da S. Almeida, M. A. Sprague-Piercy, G. A. Spyroulias, S. Sreeramulu, J. N. Tants, K. Tārs, F. Torres, S. Töws, M. Treviño, S. Trucks, A. C. Tsika, K. Varga, Y. Wang, M. E. Weber, J. E. Weigand, C. Wiedemann, J. Wirmer-Bartoschek, M. A. Wirtz Martin, J. Zehnder, M. Hengesbach, A. Schlundt, *Frontiers in Molecular Biosciences* **2021**, *8*, 89.

[52] S. Sreeramulu, C. Richter, H. Berg, M. A. Wirtz Martin, B. Ceylan, T. Matzel, J. Adam, N. Altincekic, K. Azzaoui, J. K. Bains, M. J. J. Blommers, J. Ferner, B. Fürtig, M. Göbel, J. T. Grün, M. Hengesbach, K. F. Hohmann, D. Hymon, B. Knezic, J. N. Martins, K. R. Mertinkus, A. Niesteruk, S. A. Peter, D. J. Pyper, N. S. Qureshi, U. Scheffer, A. Schlundt, R. Schnieders, E. Stirnal, A. Sudakov, A. Tröster, J. Vögele, A. Wacker, J. E. Weigand, J. Wirmer-Bartoschek, J. Wöhnert, H. Schwalbe, *Angewandte Chemie - International Edition* **2021**, *60*, 19191-19200, DOI 10.1002/anie.202103693.

[53] D. Kozakov, L. E. Grove, D. R. Hall, T. Bohnuud, S. E. Mottarella, L. Luo, B. Xia, D. Beglov, S. Vajda, *Nature Protocols* **2015**, *10*, 733–755.

[54] A. Douangamath, D. Fearon, P. Gehrtz, T. Krojer, P. Lukacik, C. D. Owen, E. Resnick, C. Strain-Damerell, A. Aimon, P. Ábrányi-Balogh, J. Brandão-Neto, A. Carbery, G. Davison, A. Dias, T. D. Downes, L. Dunnett, M. Fairhead, J. D. Firth, S. P. Jones, A. Keeley, G. M. Keserü, H. F. Klein, M. P. Martin, M. E. M. Noble, P. O'Brien, A. Powell, R. N. Reddi, R. Skyner, M. Snee, M. J. Waring, C. Wild, N. London, F. von Delft, M. A. Walsh, *Nature Communications* **2020**, *11*, DOI 10.1038/s41467-020-18709-w.

[55] D. Shin, R. Mukherjee, D. Grewe, D. Bojkova, K. Baek, A. Bhattacharya, L. Schulz, M. Widera, A. R. Mehdipour, G. Tascher, P. P. Geurink, A. Wilhelm, G. J. van der Heden van Noort, H. Ovaa, S. Müller, K.-P. Knobeloch, K. Rajalingam, B. A. Schulman, J. Cinatl, G. Hummer, S. Ciesek, I. Dikic, *Nature* **2020**, *587*, 657–662.

[56] K. Anand, J. Ziebuhr, P. Wadhwani, J. R. Mesters, R. Hilgenfeld, *Science (1979)* **2003**, *300*, 1763–1767.

[57] N. T. Nashed, A. Aniana, R. Ghirlando, S. C. Chiliveri, J. M. Louis, *Communications Biology* **2022**, *5*, 160.

[58] B. Goyal, D. Goyal, *ACS Combinatorial Science* **2020**, *22*, 297–305.

[59] O. B. Cox, T. Krojer, P. Collins, O. Monteiro, R. Talon, A. Bradley, O. Fedorov, J. Amin, B. D. Marsden, J. Spencer, F. von Delft, P. E. Brennan, *Chemical Science* **2016**, *7*, 2322-2330, DOI 10.1039/c5sc03115j.

[60] S. Sreeramulu, C. Richter, T. Kuehn, K. Azzaoui, M. J. J. Blommers, R. del Conte, M. Fragai, N. Trieloff, P. Schmieder, M. Nazaré, E. Specker, V. Ivanov, H. Oschkinat, L. Banci, H. Schwalbe, *Journal of Biomolecular NMR* **2020**, *74*, 555-563, DOI 10.1007/s10858-020-00327-9.

[61] H. Berg, M. A. Wirtz Martin, A. Niesteruk, C. Richter, S. Sreeramulu, H. Schwalbe, *Journal of Visualized Experiments* **2021**, *172*, e62262, DOI 10.3791/62262.

[62] A. J. Robertson, J. Ying, A. Bax, *Magnetic Resonance* **2021**, *2*, 129–138.

[63] R. A. Laskowski, J. Jabłońska, L. Pravda, R. S. Vařeková, J. M. Thornton, *Protein Science* **2018**, *27*, 129–134.

[64] A. Grosdidier, V. Zoete, O. Michielin, *Journal of Computational Chemistry* **2011**, *32*, 2149–2159.

[65] A. Grosdidier, V. Zoete, O. Michielin, *Nucleic Acids Research* **2011**, *39*, W270–W277.

[66] N. Kubatova, N. S. Qureshi, N. Altincekic, R. Abele, J. K. Bains, B. Ceylan, J. Ferner, C. Fuks, B. Hargittay, M. T. Hutchison, V. de Jesus, F. Kutz, M. A. Wirtz Martin, N. Meiser, V. Linhard, D. J. Pyper, S. Trucks, B. Fürtig, M. Hengesbach, F. Löhr, C. Richter, K. Saxena, A. Schlundt, H. Schwalbe, S. Sreeramulu, A. Wacker, J. E. Weigand, J. Wirmer-Bartoschek, J. Wöhnert, *Biomolecular NMR Assignments* **2021**, *15*, 65–71.

[67] D. Mendez, A. Gaulton, A. P. Bento, J. Chambers, M. De Veij, E. Félix, M. P. Magariños, J. F. Mosquera, P. Mutowo, M. Nowotka, M. Gordillo-Marañón, F. Hunter, L. Junco, G. Mugumbate, M. Rodriguez-Lopez, F. Atkinson, N. Bosc, C. J. Radoux, A. Segura-Cabrera, A. Hersey, A. R. Leach, *Nucleic Acids Research* **2019**, *47*, D930–D940.

[68] S. Kim, J. Chen, T. Cheng, A. Gindulyte, J. He, S. He, Q. Li, B. A. Shoemaker, P. A. Thiessen, B. Yu, L. Zaslavsky, J. Zhang, E. E. Bolton, *Nucleic Acids Research* **2021**, *49*, D1388–D1395.

[69] X. Chen, C. H. Reynolds, *Journal of Chemical Information and Computer Sciences* **2002**, *42*, 1407–1414.

[70] M. Kuzikov, E. Costanzi, J. Reinshagen, F. Esposito, L. Vangeel, M. Wolf, B. Ellinger, C. Claussen, G. Geisslinger, A. Corona, D. Iaconis, C. Talarico, C. Manelfi, R. Cannalire, G. Rossetti, J. Gossen, S. Albani, F. Musiani, K. Herzog, Y. Ye, B. Giabbai, N. Demitri, D. Jochmans, S. de Jonghe, J. Rymenants, V. Summa, E. Tramontano, A. R. Beccari, P. Leyssen, P. Storici, J. Neyts, P. Gribbon, A. Zaliani, *ACS Pharmacology & Translational Science* **2021**, *4*, 1096–1110.

[71] S. Jeon, M. Ko, J. Lee, I. Choi, S. Y. Byun, S. Park, D. Shum, S. Kim, *Antimicrobial Agents and Chemotherapy* **2020**, *64*, DOI 10.1128/AAC.00819-20.